J. Quant. Spectrosc. Radiat. Transfer. Vol. 10, pp. 1011–1063. Pergamon Press 1970. Printed in Great Britain

HYDROGEN STARK BROADENING CALCULATIONS WITH THE UNIFIED CLASSICAL PATH THEORY*

C. R. VIDAL, J. COOPER† and E. W. SMITH

National Bureau of Standards, Boulder, Colorado 80302

(*Received* 15 *January* 1970)

Abstract—The unified theory has been generalized for the case of upper and lower state interaction by introducing a more compact tetradic notation. The general result is then applied to the Stark broadening of hydrogen. The thermal average of the time development operator for upper and lower state interaction is presented. Except for the time ordering it contains the effect of finite interaction time between the radiator and perturbers to all orders, thus avoiding a Lewis type cutoff. A simple technique for evaluating the Fourier transform of the thermal average has been developed. The final calculations based on the unified theory and on the one-electron theory are compared with measurements in the high and low electron density regime. The unified theory calculations cover the entire line profile from the line center to the static wing and the simpler one-electron theory calculations provide the line intensities only in the line wings.

1. INTRODUCTION

FOR THE first few Balmer lines of hydrogen, recent papers (GERARDO and HILL, 1966; BACON and EDWARDS, 1968; KEPPLE and GRIEM, 1968; BIRKELAND, OSS and BRAUN, 1969) have demonstrated fairly good agreement between measurements in high electron density plasmas ($n_e > 10^{16}\,\mathrm{cm}^{-3}$) and improved calculations of the so called "modified impact theory". The experimental and theoretical half-widths differ less than about 10 per cent. However, measurements of the Lyman-α wings (BOLDT and COOPER, 1964; ELTON and GRIEM, 1964) and low electron density measurements ($n_e \cong 10^{13}\,\mathrm{cm}^{-3}$) of the higher Balmer and Paschen lines (FERGUSON and SCHLÜTER, 1963; VIDAL, 1964; VIDAL, 1965) have revealed parts of the hydrogen line profile, for which the modified impact theory appears to break down. For the higher series members better agreement has been obtained with quasi-static calculations (VIDAL, 1965). The reason the current impact theories break down is that these theories correct the completed collision assumption by means of the Lewis cutoff (LEWIS, 1961) which is only correct to second order. With this cutoff it was possible to extend the range of validity for the impact theory beyond the plasma frequency. However, in the distant wings, where the electron broadening becomes quasistatic, the second order perturbation treatment with the Lewis cutoff breaks down because the time development

* This research was supported in part by the Advanced Research Projects Agency of the Department of Defense, monitored by Army Research Office—Durham under Contract No. DA-31-124-ARO-D-139.

† Also at the Joint Institute for Laboratory Astrophysics and Dept. of Physics and Astrophysics, University of Colorado.

operator must then be evaluated to all orders. Attempts to correct the second order theory have been made already (GRIEM, 1965; SHEN and COOPER, 1969), but these theories still make the completed collision assumption by replacing the time development operator by the corresponding S-matrix, and so it has to be emphasized that in conjunction with the Lewis cutoff these theories would only be correct to second order. The impact theory in its present form is intrinsicly not able to describe the static wing and the transition region to the line center where dynamic effects cannot be neglected. To overcome this problem, several semiempirical procedures (GRIEM, 1962; GRIEM, 1967a; EDMONDS, SCHLÜTER and WELLS, 1967) have been suggested to generate a smooth transition from the modified impact theory to the static wing, which, however, all suffer from the fact that the final profile is not necessarily normalized.

Recently the classical path methods in line broadening have been reinvestigated in two review papers (SMITH, VIDAL and COOPER, 1969a, 1969b), which are from now on referred to as papers I and II. The purpose of I and II was to state clearly the different approximations which are required to obtain the classical path theories of line broadening and to find out where these theories are susceptible to improvements. In a manner similar to the Mozer–Baranger treatment of electric microfield distribution functions (BARANGER and MOZER, 1959, 1960), it was shown that the general thermal average can be expanded in two ways, one of which leads to the familiar impact theory describing the line center (BARANGER, 1958, 1962; GRIEM, KOLB and SHEN, 1959, 1962). The other expansion represents a generalized version of the one electron theory (COOPER, 1966), which holds in the line wings. It is also shown that there is generally a considerable domain of overlap between the modified impact theory and the one electron theory. Based on these results, a "unified theory" was then developed (SMITH, COOPER and VIDAL, 1969), henceforth referred to as paper III, which presents the first line shape expression which is valid from the line center out to the static line wing including the problematic transition region. The line shape obtained by the unified theory has the form

$$I(\omega) = \frac{1}{\pi} \sum Im \left\{ \mathbf{d} \frac{1}{\Delta\omega - \mathscr{L}(\Delta\omega)} \mathbf{d} \right\}, \tag{I.1}$$

where d, $\Delta\omega$, and $\mathscr{L}(\Delta\omega)$ are operators. In paper III, it was shown that the familiar impact theories, which hold in the line center, may be obtained by making a Markoff approximation in the unified theory, while the one electron theory describing the line wings is just a wing expansion of the unified theory. Consequently the crucial problem for any line broadening calculation is to evaluate the matrix elements of $\mathscr{L}(\Delta\omega)$, which is essentially the Fourier transform of the thermal average (see equations (46) and (47) of paper III). This will be done in detail in this paper for the general case of upper and lower state interactions.

Recently, another unified approach to Stark broadening has been presented by VOSLAMBER, 1969, which is formally equivalent to our results in paper III. However, the approximations to the time development operator are different as explained in more detail at the end of Section VI. His final numerical calculations are restricted to the wings of Lyman-α neglecting the influence of the ion fields on the electron broadening and thereby avoiding the ion microfield average of the electron contribution.

In the following Section II, we start with a brief summary of the basic relations which are required for the classical path approach pursued here. We then generalize the results of the unified theory to include lower state interaction (Section IV) after introducing a more

compact tetradic notation (Section III). From this general result we turn to the specific problem of hydrogen by discussing briefly the no quenching assumption (Section V) and deriving the thermal average $\mathscr{F}^{(1)}(t)$ (see equation (47) of paper III) for the general case of upper and lower state interaction (Section VI). We next investigate the multipole expansion of the classical interaction potential in the time development operator (Section VII). The thermal average $\mathscr{F}^{(1)}(t)$ is then evaluated in two steps by first performing a spherical average (Section VIII) and then an average over the collision parameters: some reference time t_0, impact parameter ρ and velocity v (Section IX). The large time limit of the thermal average, which leads to the familiar impact theories in the line center, is investigated in detail in the Appendix for different cutoff procedures and compared with the results in the literature. In Section X, a method is developed for performing the Fourier transformation of the thermal average and it leads us to the crucial function for any classical path theory of Stark broadening. This function is finally applied in Section XI to the one electron theory, which forms the basis for the asymptotic wing expansion, and in Section XII to the unified theory, which describes the whole line profile from the line center to the static wing. Numerical results are given for the hydrogen line profiles as measured by BOLDT and COOPER, 1964; ELTON and GRIEM, 1964, and VIDAL, 1964, 1965. The numerical calculations of the thermal average have been performed for the general case including lower state interactions, while the unified theory calculations have so far been restricted to the Lyman lines. The extension of the unified theory calculations to the general case is in process. The computer programs which have been used are presented in an NBS Monograph (VIDAL, COOPER and SMITH, 1970).

II. BASIC RELATIONS

In this section we will briefly outline the basic relations which are used in our classical path treatment of line broadening.

As discussed in Section 2 of paper I, we are considering a system containing a single radiator and a gas of electrons and ions. We will make the usual quasi-static approximation for the ions by regarding their electric field ε_i as being constant during the times of interest $\simeq 1/\Delta\omega$. This approximation is usually very good because the region where ion dynamics are important is normally well inside the half width of the line except for a few cases such as the n-α lines of hydrogen (GRIEM, 1967b). The complete line profile $I(\omega)$ is then given by the microfield average (see equation (3) of paper II).

$$I(\omega) = \int_0^\infty P(\varepsilon_i) I(\omega, \varepsilon_i)\, \mathrm{d}\varepsilon_i \tag{II.1}$$

where the normalized distribution function $P(\varepsilon_i)$ is the low frequency component of the fluctuating electric microfields. Due to shielding effects $P(\varepsilon_i)$ depends on the shielding parameter r_0/D where r_0 and D are the mean particle distance and the Debye length (for electrons only) respectively.

With the static ion approximation we have reduced the problem to a calculation of the electron broadening of a radiator in a static electric field ε_i. The resulting line profile $I(\omega, \varepsilon_i)$ is then simply averaged over all possible ion fields to give the complete line profile $I(\omega)$. The static ion field will be used to define the z-axis for the radiator and the ion-radiator

interaction will be taken to be the dipole interaction $eZ\varepsilon_i$ where $-eZ$ denotes the Z-component of the radiators dipole moment.

If the unperturbed radiator is described by a Hamiltonian H_a, we may then define a Hamiltonian for a radiator in the static field ε_i by

$$H_0 = H_a + eZ\varepsilon_i. \tag{II.2}$$

The complete Hamiltonian for the system is then given by

$$H = H_0 + V_e(\mathbf{R}, \mathbf{x}, \mathbf{v}, t) \tag{II.3}$$

where V_e denotes the electron radiator interaction. In this equation, $\mathbf{x}$ and $\mathbf{v}$ are $3N$ vectors $\mathbf{x} = (\mathbf{x}_1, \mathbf{x}_2, \ldots, \mathbf{x}_N)$, $\mathbf{v} = (\mathbf{v}_1, \mathbf{v}_2, \ldots, \mathbf{v}_N)$, which denote the positions and velocities of the N electrons and $\mathbf{R}$ denotes some internal radiator coordinates. For one-electron atoms, $\mathbf{R}$ is the position of the "orbital" electron relative to the nucleus. The interaction V_e will be regarded as a sum of binary interactions,

$$V_e(\mathbf{R}, \mathbf{x}, \mathbf{v}, t) = \sum_j V_1(\mathbf{R}, \mathbf{x}_j, \mathbf{v}_j, t) \tag{II.4}$$

where V_1 denotes the interaction between the radiator and a single electron. As is well known the line shape $I(\omega, \varepsilon_i)$ may be given by the Fourier transform of an autocorrelation function $C(t)$ (BARANGER, 1962)

$$I(\omega, \varepsilon_i) = \frac{1}{\pi} Re \int_0^\infty e^{i\omega t} C(t)\, dt. \tag{II.5}$$

In the classical path approximation, the correlation function for electric dipole radiation is given by

$$C(t) = Tr_a\{\mathbf{d}\langle T_a^\dagger(t)\mathbf{d}T_a(t)\rangle_{av}\rho_a\}, \tag{II.6}$$

where $\mathbf{d}$ and ρ_a denote the dipole moment and the density matrix for the radiator. The thermal average denoted by the subscript av represents the average over electron states (see equation (47) of paper I):

$$\langle T_a^\dagger(t)\mathbf{d}T_a(t)\rangle_{av} = \int d\mathbf{x}\, d\mathbf{v} P(\mathbf{x}) W(\mathbf{v}) T_a^\dagger(\mathbf{R}, \mathbf{x}, \mathbf{v}, t)\mathbf{d}T_a(\mathbf{R}, \mathbf{x}, \mathbf{v}, t) \tag{II.7}$$

where $P(\mathbf{x})$ and $W(\mathbf{v})$ are the position and velocity distribution functions for the electron perturbers (defined by equations (37) to (40) in paper II). The time development operator for the system $T_a(\mathbf{R}, \mathbf{x}, \mathbf{v}, t)$ is the solution of the differential equation

$$i\hbar \frac{\partial}{\partial t} T_a(t) = [H_0 + V_e(t)] T_a(t) \tag{II.8}$$

and it may be written in an interaction representation defined by

$$T_a(\mathbf{R}, \mathbf{x}, \mathbf{v}, t) = \exp(-itH_0/\hbar) U_a(\mathbf{R}, \mathbf{x}, \mathbf{v}, t) \tag{II.9}$$

where

$$i\hbar \frac{\partial}{\partial t} U_a(t) = \tilde{V}_e(t) U_a(t) \tag{II.10}$$

and

$$\tilde{V}_e(t) = \exp(itH_0/\hbar)V_e(t)\exp(-itH_0/\hbar). \tag{II.11}$$

It should be noted that $\tilde{V}_e(t)$ is identical with $\tilde{V}_e(t)$ in paper II except that we have not yet made the no quenching assumption which removes the unperturbed part H_a in the Hamiltonian H_0 in equation (II.11). Using the time ordering operator $\mathcal{O}$, $U_a(t)$ may be written in the form

$$U_a(\mathbf{R}, \mathbf{x}, \mathbf{v}, t) = \mathcal{O}\exp\left\{-\frac{i}{\hbar}\int_0^t \tilde{V}_e(\mathbf{R}, \mathbf{x}, \mathbf{v}, t')\,dt'\right\}. \tag{II.12}$$

To evaluate the trace over atomic states in equation (II.6), it is convenient to use the H_0 eigenstates $|a\rangle, |b\rangle, \ldots$ with the eigenvalues $E_a, E_b, \ldots$. Hence, using $U_a(t)$ we have

$$C(t) = \sum_{abcd} \langle a|\mathbf{d}|b\rangle\langle c|\mathbf{d}|d\rangle\, e^{-i\omega_{dc}t} \tag{II.13}$$

$$[\langle b|U_a^\dagger(t)|c\rangle\langle d|U_a(t)|a\rangle]_{av}\langle a|\rho_a|a\rangle$$

where

$$\omega_{dc} = (E_d - E_c)/\hbar. \tag{II.14}$$

In paper II and III, the correlation function $C(t)$ was evaluated for the case of no lower state interactions in order to keep the mathematics as simple as possible because one of the $U_a(t)$ operators in equation (II.13) may then be replaced by a unit operator. In this paper we will give a more general evaluation of $C(t)$ which includes lower state interactions. For this purpose we introduce in the next section a more compact tetradic notation. Furthermore, it should be noted already at this stage that we will interchange the sequence of approximations with respect to paper II by deriving the generalized unified theory before making the no quenching approximation. This makes the results of the unified theory also useful for situations where the no quenching approximation cannot be made like, for example, microwave lines.

III. THE TETRADIC NOTATION

The purpose of the tetradic notation which we shall use is to write the product of the $U_a(t)$ operators in equation (II.13) in terms of a single operator. To do this we first consider the product of the matrix elements $\langle\alpha|A|\alpha'\rangle$ and $\langle\beta|B|\beta'\rangle$ where A and B may be any arbitrary operator. This product may be written in terms of the direct product $A \otimes B$ according to

$$\langle\alpha|A|\alpha'\rangle\langle\beta|B|\beta'\rangle \equiv \langle\alpha\beta|A\otimes B|\alpha'\beta'\rangle, \tag{III.1}$$

where the product states $|\alpha\beta\rangle = |\alpha\rangle|\beta\rangle$ are essentially the same as the states of Baranger's "doubled atom" (BARANGER, 1962). This direct product, $A\otimes B$, is a simple form of tetradic operator. If one of the operators A or B happens to be a unit operator I, we may conveniently denote this fact by means of superscripts l and r according to

$$\langle\alpha\beta|A\otimes I|\alpha'\beta'\rangle = \langle\alpha\beta|A^l|\alpha'\beta'\rangle = \langle\alpha|A|\alpha'\rangle\delta_{\beta\beta'} \tag{III.2}$$

$$\langle\alpha\beta|I\otimes B|\alpha'\beta'\rangle = \langle\alpha\beta|B^r|\alpha'\beta'\rangle = \langle\beta|B|\beta'\rangle\delta_{\alpha\alpha'} \tag{III.3}$$

That is, a superscript l denotes a "left" operator which operates only on the "left" subspace (in this case the $|\alpha\rangle, |\alpha'\rangle$ subspace) and a superscript r denotes a "right" operator which operates on the "right" subspace. It thus is clear that any "left" operator will commute with any "right" operator:

$$[A^l, B^r] = 0. \tag{III.4}$$

With this notation, the thermal average in equation (II.13) can now be written in the more compact form

$$\begin{aligned}[\langle b|U_a^\dagger(t)|c\rangle\langle d|U_a(t)|a\rangle]_{\text{av}} &= [\langle c|U_a^*(t)|b\rangle\langle d|U_a(t)|a\rangle]_{\text{av}} \\ &= [\langle cd|U_a^{l*}(t)U_a^r|ba\rangle]_{\text{av}} \\ &= \langle cd|[U_a^{l*}(t)U_a^r(t)]_{\text{av}}|ba\rangle.\end{aligned} \tag{III.5}$$

We have chosen to write $\langle b|U_a^\dagger(t)|c\rangle$ as $\langle c|U_a^*(t)|b\rangle$ simply for convenience in the derivation given in later sections. Noting the definition of $U_a(t)$ given in equation (II.12), we define operators $\tilde{V}_e^l(\mathbf{R}, \mathbf{x}, \mathbf{v}, t)$ and $\tilde{V}_e^r(\mathbf{R}, \mathbf{x}, \mathbf{v}, t)$ so that

$$\begin{aligned}U_a^l(\mathbf{R}, \mathbf{x}, \mathbf{v}, t) &= \mathcal{O} \exp\left\{-\frac{i}{\hbar}\int_0^t \tilde{V}_e^l(\mathbf{R}, \mathbf{x}, \mathbf{v}, t')\,dt'\right\} \\ U_a^r(\mathbf{R}, \mathbf{x}, \mathbf{v}, t) &= \mathcal{O} \exp\left\{-\frac{i}{\hbar}\int_0^t \tilde{V}_e^r(\mathbf{R}, \mathbf{x}, \mathbf{v}, t')\,dt'\right\}.\end{aligned} \tag{III.6}$$

Since any "left" operator commutes with any "right" operator, we have

$$\begin{aligned}U_a^{l*}(\mathbf{R}, \mathbf{x}, \mathbf{v}, t)U_a^r(\mathbf{R}, \mathbf{x}, \mathbf{v}, t) &= \mathcal{O} \exp\left\{-\frac{i}{\hbar}\int_0^t \tilde{\mathscr{V}}_e(\mathbf{R}, \mathbf{x}, \mathbf{v}, t')\,dt'\right\} \\ &\equiv \mathscr{U}(\mathbf{R}, \mathbf{x}, \mathbf{v}, t)\end{aligned} \tag{III.7}$$

where

$$\tilde{\mathscr{V}}_e(\mathbf{R}, \mathbf{x}, \mathbf{v}, t) = \tilde{V}_e^r(\mathbf{R}, \mathbf{x}, \mathbf{v}, t) - \tilde{V}_e^{l*}(\mathbf{R}, \mathbf{x}, \mathbf{v}, t). \tag{III.8}$$

We have now succeeded in replacing the two $U_a(t)$ operators by a more general tetradic operator $\mathscr{U}(t)$ which operates in both "left" and "right" subspaces. Equation (III.5) thus becomes

$$[\langle b|U_a^\dagger(t)|c\rangle\langle d|U_a(t)|a\rangle]_{\text{av}} = \langle cd|[\mathscr{U}(t)]_{\text{av}}|ba\rangle. \tag{III.9}$$

It is important to realize that the tetradic operator $\mathscr{U}(t)$ is *formally* the same as the operator $U_a(t)$; that is, it satisfies the same type of differential equation

$$i\hbar\frac{\partial}{\partial t}\mathscr{U}(\mathbf{R}, \mathbf{x}, \mathbf{v}, t) = \tilde{\mathscr{V}}_e(\mathbf{R}, \mathbf{x}, \mathbf{v}, t)\mathscr{U}(\mathbf{R}, \mathbf{x}, \mathbf{v}, t). \tag{III.10}$$

This means that all of the line broadening formalism which has been developed for $U_a(t)$, will be directly applicable to $\mathscr{U}(t)$.

To make the formal correspondence more complete we use the operators H_0^l, H_0^r, $V_e^l(\mathbf{R}, \mathbf{x}, \mathbf{v}, t)$ and $V_e^r(\mathbf{R}, \mathbf{x}, \mathbf{v}, t)$ to define the tetradics $\mathscr{H}_0$ and $\mathscr{V}_e(\mathbf{R}, \mathbf{x}, \mathbf{v}, t)$ according to

$$\mathscr{H}_0 = H_0^r - H_0^l \tag{III.11}$$

$$\mathscr{V}_e(\mathbf{R}, \mathbf{x}, \mathbf{v}, t) = V_e^r(\mathbf{R}, \mathbf{x}, \mathbf{v}, t) - V_e^{l*}(\mathbf{R}, \mathbf{x}, \mathbf{v}, t). \tag{III.12}$$

Since any left operator commutes with any right operator we have

$$\begin{aligned}\tilde{V}_e^r(t) &= \exp\{itH_0^r/\hbar\} V_e^r(t) \exp\{-itH_0^r/\hbar\} \\ &= \exp\{it\mathscr{H}_0/\hbar\} V_e^r(t) \exp\{-it\mathscr{H}_0/\hbar\}.\end{aligned} \tag{III.13}$$

Hence

$$\tilde{\mathscr{V}}_e(\mathbf{R}, \mathbf{x}, \mathbf{v}, t) = \exp\{it\mathscr{H}_0/\hbar\} \mathscr{V}_e(\mathbf{R}, \mathbf{x}, \mathbf{v}, t) \exp\{-it\mathscr{H}_0/\hbar\} \tag{III.14}$$

which is formally the same as equation (II.11). It is also obvious that both $\mathscr{V}_e$ and $\tilde{\mathscr{V}}_e$ will be given by a sum over binary interactions $\mathscr{V}_1$ or $\tilde{\mathscr{V}}_1$ just as in equation (II.4).

$$\mathscr{V}_e(\mathbf{R}, \mathbf{x}, \mathbf{v}, t) = \sum_j \mathscr{V}_1(\mathbf{R}, \mathbf{x}_j, \mathbf{v}_j, t) \tag{III.15}$$

$$\mathscr{V}_1(\mathbf{R}, \mathbf{x}_j, \mathbf{v}_j, t) = V_1^r(\mathbf{R}, \mathbf{x}_j, \mathbf{v}_j, t) - V_1^{l*}(\mathbf{R}, \mathbf{x}_j, \mathbf{v}_j, t) \tag{III.16}$$

The formal similarity between the operators H_0, $V_e(t)$, $\tilde{V}_e(t)$, $U_a(t)$, etc. and the tetradic operators $\mathscr{H}_0$, $\mathscr{V}_e(t)$, $\tilde{\mathscr{V}}_e(t)$, $\mathscr{U}(t)$, etc. will greatly simplify the treatment of the thermal average for the general case of upper and lower state interactions.

IV. THE GENERALIZED UNIFIED THEORY

Using the tetradic operators as defined in the previous section we have for the correlation function

$$\begin{aligned}C(t) = \sum_{abcd} &\langle a|\mathbf{d}|b\rangle\langle c|\mathbf{d}|d\rangle e^{-i\omega_{ac}t}\langle a|\rho_a|a\rangle \\ &\langle cd|\bar{\mathscr{F}}(t)|ba\rangle\end{aligned} \tag{IV.1}$$

where $\bar{\mathscr{F}}(t)$ denotes the thermal average of $\mathscr{U}(\mathbf{R}, \mathbf{x}, \mathbf{v}, t)$:

$$\begin{aligned}\bar{\mathscr{F}}(t) &= [\mathscr{U}(t)]_{\text{av}} \\ &= \int d\mathbf{x}\, d\mathbf{v} P(\mathbf{x}) W(\mathbf{v}) \mathscr{U}(\mathbf{R}, \mathbf{x}, \mathbf{v}, t).\end{aligned} \tag{IV.2}$$

This tetradic operator $\bar{\mathscr{F}}(t)$ is formally identical to the operator $F(t)$ defined in Section (2.A) of paper III. It would also be formally identical to the $F(t)$ defined by equation (19) of paper II if we would make the no quenching approximation at this point. To preserve generality, however, the no quenching approximation will be deferred until a later section when we specify the $|a\rangle, |b\rangle, \ldots$ eigenstates to be H_0 eigenstates for hydrogen.

Following the formalism developed in Section 2 of paper III, we define an operator $\mathscr{F}(\mathbf{R}, \mathbf{x}, \mathbf{v}, t)$ by

$$\mathscr{F}(\mathbf{R}, \mathbf{x}, \mathbf{v}, t) = P(\mathbf{x}) W(\mathbf{v}) \mathscr{U}(\mathbf{R}, \mathbf{x}, \mathbf{v}, t) \tag{IV.3}$$

so that

$$\bar{\mathscr{F}}(t) = \int \mathrm{d}\mathbf{x}\,\mathrm{d}\mathbf{v}\mathscr{F}(\mathbf{R}, \mathbf{x}, \mathbf{v}, t) \tag{IV.4}$$

(cf. equations (11) and (12) of paper III). From equation (III.10) we see that

$$i\hbar\frac{\partial}{\partial t}\mathscr{F}(\mathbf{R}, \mathbf{x}, \mathbf{v}, t) = \tilde{\mathscr{V}}_e(\mathbf{R}, \mathbf{x}, \mathbf{v}, t)\mathscr{F}(\mathbf{R}, \mathbf{x}, \mathbf{v}, t) \tag{IV.5}$$

which is formally the same as equation (13) in paper III. We next introduce a projection operator $\mathscr{P}$ which is identically the same as the operator $\mathscr{P}$ defined by equation (14) of paper III (the fact that $\mathscr{P}$ now operates on tetradics does not change its definition). That is, for *any* function of electron variables $f(\mathbf{x}, \mathbf{v})$ we have

$$\mathscr{P}f(\mathbf{x}, \mathbf{v}) = P(\mathbf{x})W(\mathbf{v})\int \mathrm{d}\mathbf{x}'\,\mathrm{d}\mathbf{v}'f(\mathbf{x}', \mathbf{v}'). \tag{IV.6}$$

This relation holds whether f is a matrix, tetradic or any other type of operator. With this operator we can follow the derivation in Section (2.B) of paper III replacing H_0, V_e, $\tilde{V}_e$ etc. by $\mathscr{H}_0$, $\mathscr{V}_e$, $\tilde{\mathscr{V}}_e$, etc. As a result (cf. equation (27) in paper III) we have

$$\frac{\partial}{\partial t}\bar{\mathscr{F}}(t) = -\hbar^{-2}\int_0^t \exp(it'\mathscr{H}_0/\hbar)[\tilde{\mathscr{V}}_e(t-t')\mathscr{G}(t-t')\tilde{\mathscr{V}}_e(0)]_{\mathrm{av}}$$
$$\exp(-it'\mathscr{H}_0/\hbar)\bar{\mathscr{F}}(t')\,\mathrm{d}t' \tag{IV.7}$$

where

$$\mathscr{G}(\mathbf{R}, \mathbf{x}, \mathbf{v}, t-t') = \mathscr{O}\exp\left\{-\frac{i}{\hbar}\int_0^{t-t'}(1-\mathscr{P})\tilde{\mathscr{V}}_e(\mathbf{R}, \mathbf{x}, \mathbf{v}, t'')\,\mathrm{d}t''\right\}. \tag{IV.8}$$

Returning to equations (II.5) and (IV.1) we see that the quantity of interest is not $\bar{\mathscr{F}}(t)$ but rather its Fourier transform.

$$\begin{aligned}\langle cd|\mathscr{I}(\omega)|ba\rangle &= \int_0^\infty \mathrm{e}^{i\omega t}\,\mathrm{e}^{-i\omega_{dc}t}\langle cd|\bar{\mathscr{F}}(t)|ba\rangle\,\mathrm{d}t \\ &= \int_0^\infty \mathrm{e}^{i\omega t}\langle cd|\exp(-it\mathscr{H}_0/\hbar)\bar{\mathscr{F}}(t)|ba\rangle\,\mathrm{d}t \\ &= \int_0^\infty \mathrm{e}^{i\omega t}\langle cd|\tilde{\bar{\mathscr{F}}}(t)|ba\rangle\,\mathrm{d}t\end{aligned} \tag{IV.9}$$

where

$$\tilde{\bar{\mathscr{F}}}(t) = \exp(-it\mathscr{H}_0/\hbar)\bar{\mathscr{F}}(t). \tag{IV.10}$$

From equation (IV.7) we see that

$$\frac{\partial}{\partial t}\tilde{\mathscr{F}}(t) = -(i\mathscr{H}_0/\hbar)\tilde{\mathscr{F}}(t) - \hbar^{-2}\int_0^t \exp(-i(t-t')\mathscr{H}_0/\hbar)$$
$$[\tilde{\mathscr{V}}_e(t-t')\mathscr{G}(t-t')\tilde{\mathscr{V}}_e(0)]_{\mathrm{av}}\tilde{\mathscr{F}}(t')\,\mathrm{d}t'. \tag{IV.11}$$

Solving this equation by Fourier transforms gives

$$\mathscr{I}(\omega) = i[\Delta\omega_{\mathrm{op}} - \mathscr{L}(\Delta\omega_{\mathrm{op}})]^{-1} \tag{IV.12}$$

where

$$\mathscr{L}(\Delta\omega_{\mathrm{op}}) = -i\hbar^{-2}\int_0^\infty \exp(it\Delta\omega_{\mathrm{op}})[\tilde{\mathscr{V}}_e(t)\mathscr{G}(t)\tilde{\mathscr{V}}_e(0)]_{\mathrm{av}}\,\mathrm{d}t \tag{IV.13}$$

and $\Delta\omega_{\mathrm{op}}$ is an operator defined by

$$\Delta\omega_{\mathrm{op}} = \omega - \mathscr{H}_0/\hbar = \omega - (H_0^r - H_0^l)/\hbar. \tag{IV.14}$$

With these results, the line shape given in equation (II.5) becomes (cf. equation (I.1))

$$I(\omega, \varepsilon_i) = \frac{1}{\pi} Im \sum_{abcd} \langle a|\mathbf{d}|b\rangle\langle c|\mathbf{d}|d\rangle\langle a|\,\rho_a|a\rangle$$
$$\langle cd|[\Delta\omega_{\mathrm{op}} - \mathscr{L}(\Delta\omega_{\mathrm{op}})]^{-1}|ba\rangle. \tag{IV.15}$$

We next simplify $\mathscr{L}(\Delta\omega_{\mathrm{op}})$ by means of the impact approximation (see Section (3.2) of paper II). Basically this approximation assumes that the average collision is weak, that strong collisions do not overlap in time and that a weak collision overlapping a strong one is negligible in comparison (weak collisions are those interactions for which a low order perturbation expansion in $\mathscr{V}_e$ provides a good approximation to $\mathscr{U}$ or $\mathscr{G}$; for strong collisions the full exponential must be retained). It should be emphasized again that we make a distinction between the impact *approximation* and the impact *theory*. The latter contains the impact approximation as weli as other approximations like the completed collision assumption which will not be made here. We also assume that the electron perturbers may be replaced by statistically independent quasi particles (e.g. shielded electrons). In Section (3) and Appendix B of paper III, it is shown that these approximations reduce $\mathscr{L}(\Delta\omega_{\mathrm{op}})$ to

$$\mathscr{L}(\Delta\omega_{\mathrm{op}}) = -i\Delta\omega_{\mathrm{op}}\int_0^\infty \mathrm{e}^{it\Delta\omega_{\mathrm{op}}}\bar{\mathscr{F}}^{(1)}(t)\,\mathrm{d}t\,\Delta\omega_{\mathrm{op}} \tag{IV.16}$$

where

$$\bar{\mathscr{F}}^{(1)}(t) = n_e\int \mathrm{d}\mathbf{x}_1\,\mathrm{d}\mathbf{v}_1 W(\mathbf{v}_1)[\mathscr{U}_1(\mathbf{R}, \mathbf{x}_1, \mathbf{v}_1, t) - 1] \tag{IV.17}$$

and

$$\mathscr{U}_1(\mathbf{R}, \mathbf{x}_1, \mathbf{v}_1, t) = \mathscr{O} \exp\left\{-\frac{i}{\hbar}\int_0^t V_1(\mathbf{R}, \mathbf{x}_1, \mathbf{v}_1, t')\,dt'\right\} \tag{IV.18}$$

and n_e denotes the electron density.

Equations (IV.15) through (IV.18) give the line profile of the generalized unified theory. To obtain the impact theory we simply replace $\mathscr{L}(\Delta\omega_{op})$ by $\mathscr{L}(0)$ and as discussed in Section 4 of paper III, we have the familiar result (cf. equation (44) of BARANGER, 1962).

$$\mathscr{L}(0) = i\int (S_1^{i*}S_1^r - 1)\,dv \tag{IV.19}$$

where S_1 denotes an S-matrix for a binary (completed) collision and $\int dv$ denotes the integral over collision variables, as defined in the Appendix of paper II.

$$\int dv \equiv n_e \int_0^\infty dv\, vf(v) \int d\rho\, 2\pi\rho \int d\Omega. \tag{IV.20}$$

In comparing equation (IV.19) with Baranger's result it is important to note that Baranger's operators S_i and S_f operate only on "initial" and "final" states respectively, whereas our operators S_1^i and S_1^r operate on all possible H_0 eigenstates. This difference occurs because we have not made the no quenching assumption yet.

The other limit of the one electron theory is obtained by making a wing expansion of the unified theory; that is, the operator $[\Delta\omega_{op} - \mathscr{L}(\Delta\omega_{op})]^{-1}$ is expanded in powers of $[\mathscr{L}(\Delta\omega_{op})/\Delta\omega_{op}]$. To lowest order this gives

$$\begin{aligned}[\Delta\omega_{op} - \mathscr{L}(\Delta\omega_{op})]^{-1} &= \frac{1}{\Delta\omega_{op}} + \frac{1}{\Delta\omega_{op}}\mathscr{L}(\Delta\omega_{op})\frac{1}{\Delta\omega_{op}} + \cdots \\ &= \frac{1}{\Delta\omega_{op}} - i\int_0^\infty e^{it\Delta\omega_{op}}\bar{\mathscr{F}}^{(1)}(t)\,dt + \cdots.\end{aligned} \tag{IV.21}$$

The first term, $1/\Delta\omega_{op}$, gives a delta function when one takes the imaginary part required by equation (IV.15). To get this delta function we approximate radiation damping effects by using $(\Delta\omega_{op} + i\varepsilon)$ in place of $\Delta\omega_{op}$ (see Section (3.A) of SMITH and HOOPER, 1967); the imaginary part of $1/(\Delta\omega_{op} + i\varepsilon)$ is just $-\pi\delta(\Delta\omega_{op})$ when $\varepsilon \to 0$. When this delta function term is averaged over ion fields according to equation (II.1) it will produce the line broadening due to the static ions alone (see Section 5 of paper II). The influence of the electrons as well as electron–ion coupling is contained in the second term of equation (IV.21). Hence one is interested in the matrix elements of the Fourier transform of $\bar{\mathscr{F}}^{(1)}(t)$, which is also the quantity of interest in the unified theory (see equation (IV.16)). The primary difference between calculations made by the unified and one-electron theories is therefore the matrix inversion of $[\Delta\omega_{op} - \mathscr{L}(\Delta\omega_{op})]$ which is required by the unified theory but not by the one electron theory. Since the matrix elements of the Fourier transform of $\bar{\mathscr{F}}^{(1)}(t)$ play such a central role in any classical path theory (including the impact theory), the evaluation of these matrix elements for hydrogen will be discussed in detail in the following sections.

V. THE NO-QUENCHING APPROXIMATION FOR HYDROGEN

In the preceding section we have derived the thermal average $\bar{\mathscr{F}}(t)$ and its Fourier transform $\mathscr{I}(\omega)$ for the general case of upper and lower state interaction. In order to evaluate $I(\omega, \varepsilon_i)$ in equation (IV.15) we have to consider the complete trace over all H_0 eigenstates $|a\rangle, |b\rangle, \ldots$. However, in looking at the equations (IV.9), (IV.18) and (III.14) one realizes that due to the exponential factors only a few of all the possible matrix elements will contribute significantly to the final line profile at a particular frequency ω. That is, we can neglect those matrix elements for which the argument of the exponential factor is so large that it gives rise to rapid oscillations within the range of the time integral. Hence, if one treats well isolated lines, only those matrix elements of $U_1(t)$ between either "initial" or "final" states have to be considered. We may therefore state the no-quenching approximation as

$$\mathscr{U}_1(t) = U_1^{f*}(t)U_1^i(t) \tag{V.1}$$

where U_1 now no longer operates on the complete "left" or "right" subspace, but only on "initial" or "final" states (see also Section 2.2 and 7.2 of paper II).

Further approximations cannot easily be generalized and depend on the particular problem investigated. We now apply our general results to the problem of hydrogen. In this case the no-quenching assumption states that we need to consider only those matrix elements of $U_1(t)$ and $\tilde{V}_1(\mathbf{R}, \mathbf{x}_1, \mathbf{v}_1, t)$ which are diagonal in the principal quantum number n. As shown already in paper II this is a good approximation as long as the lines investigated are well separated. For calculating the line wings it is furthermore required that there is no appreciable overlap with wings of adjacent lines in the region of interest. The same is true also in any reliable measurement of line wings.

To show this we can proceed as in Sections 2.2 and 7.2 of paper II with the difference that now we are dealing with the operator $H_0 = H_a + eZ\varepsilon_i$ rather than just H_a. Since H_a does not commute with Z we introduce a projection operator P_n (see Section 2.2 of paper II) which picks out the part of an operator which is diagonal in n. Using this operator we split H_0 into a part which is diagonal in n

$$H_{\text{on}} = H_a + eP_nZ\varepsilon_i \tag{V.2}$$

and a part which is not diagonal in n

$$H_{\text{off}} = e(1-P_n)Z\varepsilon_i. \tag{V.3}$$

H_a now commutes with P_nZ because both operators are diagonal in parabolic coordinates. We therefore specify their eigenstates completely by the principal quantum number n, the magnetic quantum number m and the quantum number q which is defined to be

$$q = n_1 - n_2; \tag{V.4}$$

n_1 and n_2 are the usual parabolic quantum numbers which obey the relation

$$n = n_1 + n_2 + |m| + 1. \tag{V.5}$$

Knowing the solution of the eigenvalue problem

$$H_{\text{on}}|nqm\rangle = E_{nqm}|nqm\rangle \tag{V.6}$$

with

$$E_{nqm} = E_n + eZ_{nq}\varepsilon_i \tag{V.7}$$

we see from a second order perturbation approach (cf. Chapter 16 of MERZBACHER, 1961) that the energy correction

$$\Delta E^{(2)}_{nqm} = \sum_{n \neq n'} \frac{|\langle nqm|H_{\text{off}}|n'q'm'\rangle|^2}{E_{nqm} - E_{n'q'm'}} \tag{V.8}$$

can always be neglected as long as the ion fields do not become too large. This is again equivalent to stating that the lines have to be well separated.

As a result one is left with the eigenvalues $E_a, E_b, \ldots$ of the Hamiltonian H_{on} whose eigenstates $|a\rangle, |b\rangle, \ldots |d\rangle$ are the parabolic states $|nqm\rangle$. This allows us to rewrite the autocorrelation function $C(t)$ in equation (IV.1) for hydrogen in the form:

$$\begin{aligned} C(t, \varepsilon_i) = \sum \langle nq_a m_a|\mathbf{d}|n'q'_a m'_a\rangle \langle n'q'_b m'_b|\mathbf{d}|nq_b m_b\rangle \\ \times \exp\left\{-\frac{i}{\hbar}[E_n - E_{n'} + e(Z_{nq_b} - Z_{n'q'_b})\varepsilon_i]t\right\} \langle nq_a m_a|\rho_a|nq_a m_a\rangle \\ \times \langle n'q'_b m'_b; nq_b m_b|\dot{\mathscr{F}}(t)|n'q'_a m'_a; nq_a m_a\rangle \end{aligned} \tag{V.9}$$

where quantum numbers which refer to the lower state are distinguished from the upper state quantum numbers by a prime.

The matrix elements of $P_n Z$ are given by (see BETHE and SALPETER, 1957)

$$\langle nqm|Z|nqm\rangle = Z_{nq} = \tfrac{3}{2}nqa_0 \tag{V.10}$$

with $a_0 = \hbar^2/(me^2)$ being the Bohr radius. As a further definition the ion field ε_i will be normalized to the Holtsmark field strength ε_0

$$\varepsilon_i = \beta \cdot \varepsilon_0 \tag{V.11}$$

where

$$\varepsilon_0 = \left(\frac{4\pi}{3}\right)^{2/3} en_e^{2/3}. \tag{V.12}$$

This yields

$$\frac{e}{\hbar}(Z_{nq_b} - Z_{n'q'_b})\varepsilon_i = \Delta\omega_i(n, q_b, n', q'_b) \cdot \beta \tag{V.13}$$

with

$$\Delta\omega_i(n, q_b, n', q'_b) = \left(\frac{4\pi}{3}\right)^{2/3} \cdot \frac{3}{2}(nq_b - n'q'_b)\frac{\hbar}{m}n_e^{2/3}. \tag{V.14}$$

$\Delta\omega_i$ is now the frequency shift of a particular Stark component characterized by the quantum numbers n, q_b, n' and q'_b due to the Holtsmark field strength ε_0. Introducing the frequency shift $\Delta\omega = \omega - \omega_{nn'}$ where the frequency of the unperturbed line $\omega_{nn'}$ is given by

$$\omega_{nn'} = (E_n - E_{n'})/\hbar \tag{V.15}$$

the line profile $I(\Delta\omega, \beta)$ can be written in the form

$$I(\Delta\omega, \beta) = \frac{Re}{\pi} \sum \langle nq_a m_a|\mathbf{d}|n'q_a'm_a'\rangle \langle n'q_b'm_b'|\mathbf{d}|nq_b m_b\rangle \times \langle nq_a m_a|\rho_a|nq_a m_a\rangle \langle n'q_b'm_b'; nq_b m_b|\mathscr{I}(\omega)|n'q_a'm_a'; nq_a m_a\rangle \tag{V.16}$$

where

$$\langle n'q_b'm_b'; nq_b m_b|\mathscr{I}(\omega)|n'q_a'm_a'; nq_a m_a\rangle = \int_0^\infty \mathrm{d}t \exp\{i(\Delta\omega - \Delta\omega_i\beta)t\} \langle n'q_b'm_b'; nq_b m_b|\bar{\mathscr{F}}(t)|n'q_a'm_a'; nq_a m_a\rangle .$$

Performing the ion field average according to equation (II.1) will then give us the desired line profile once we know the thermal average $\bar{\mathscr{F}}(t)$.

VI. THE THERMAL AVERAGE $\bar{\mathscr{F}}^{(1)}(t)$ FOR HYDROGEN

In Section IV we saw that the crucial problem in any classical path theory of line broadening is the evaluation of the matrix elements of $\bar{\mathscr{F}}^{(1)}(t)$. With the no-quenching approximation for hydrogen a typical matrix element in parabolic states is given by

$$\langle n'q_b'm_b'; nq_b m_b|\bar{\mathscr{F}}^{(1)}(t)|n'q_a'm_a'; nq_a m_a\rangle = n_e \int \mathrm{d}\mathbf{x}_1 \, \mathrm{d}\mathbf{v}_1 W(\mathbf{v}_1) \langle n'q_b'm_b'; nq_b m_b|\mathscr{U}_1(t) - 1|n'q_a'm_a'; nq_a m_a\rangle \tag{VI.1}$$

To simplify the evaluation we transform to the natural collision variables ρ, v and t_0 which denote the impact parameter, electron velocity and some reference time of the collision (see the appendix of paper II). The orientation of the collision axes with respect to the radius vector $\mathbf{R}$ of the orbital electron is specified by the three Euler angles represented by Ω. Furthermore we assume a spherically symmetric distribution of perturbing electrons; this is a good approximation as long as the impact parameters are not too small. The velocity distribution function $W(v)$ is related to the Maxwell distribution function $f(v)$ by

$$f(v) = 4\pi v^2 W(v). \tag{VI.2}$$

With the preceding definitions equation (VI.1) can be rewritten as

$$\langle n'q_b'm_b'; nq_b m_b|\bar{\mathscr{F}}^{(1)}(t)|n'q_a'm_a'; nq_a m_a\rangle = \frac{n_e}{4\pi} \int \mathrm{d}\Omega \int \mathrm{d}v \, v f(v) \int \mathrm{d}\rho \, \rho \int \mathrm{d}t_0 \langle n'q_b'm_b'; nq_b m_b|\mathscr{U}_1(t) - 1|n'q_a'm_a'; nq_a m_a\rangle. \tag{VI.3}$$

Next we have to know the matrix elements of the time development operator $\mathscr{U}_1(t)$ defined by equation (IV.18). This requires the matrix elements of the interaction potential $\tilde{\mathscr{V}}_1(t)$. In order to save some writing we consider for the moment only $U_1(t)$ and $\tilde{V}_1(t)$ which after making the no-quenching assumption may be the "initial" or "final" part of the corresponding tetradic operators (see equation (V.1)). A typical matrix element of $\tilde{V}_1(t)$ is

given by

$$\langle nq_c m_c|\tilde{V}_1(t)|nq_d m_d\rangle = \exp\left\{i\frac{e}{\hbar}(Z_{nq_c}-Z_{nq_d})\varepsilon_i t\right\}\langle nq_c m_c|V_1(t)|nq_d m_d\rangle. \tag{VI.4}$$

With the no-quenching assumption the unperturbed energy eigenvalues E_n have cancelled. At this stage we now make another simplification by dropping the exponential in the latter equation; this has been done in all previous Stark broadening calculations but it is rarely stated explicitly. This will be a good approximation in the line wings where the time of interest $1/\Delta\omega$ are small and $\Delta\omega$ is much larger than the average ion field splitting. In the line center, however, the argument of the exponential can easily be on the order of unity or larger in which case $\tilde{V}_1(t)$ effectively vanishes due to rapid oscillations of the exponentials. This effect was first noted by VAN REGEMORTER, 1964, who shows that this effectively introduces another cutoff which may easily be smaller than the usual Debye or Lewis cutoffs. This additional cutoff has been included in recent calculations (KEPPLE and GRIEM, 1968). However, as discussed in Section XII it turns out that its influence on the final line profile is in most cases negligible.

Neglecting the ion field exponentials in equation (VI.4), the time development operator U_1 is now given by

$$U_1 = \mathcal{O}\exp\left\{-\frac{i}{\hbar}\int_0^t P_n V_1(t')\,dt'\right\} \tag{VI.5}$$

where the time ordering is still required because $P_n V_1(t)$ need not commute with $P_n V_1(t')$. In paper II it was shown that this time ordering is negligible for weak collisions (to second order) as well as quasistatic collisions (i.e. in the distant line wings). Time ordering is not negligible for strong collisions; however, when the thermal average is performed, the errors due to neglecting time ordering are expected to be small. The reason for this is that the time development operator

$$U_1 = \exp\left\{-\frac{i}{\hbar}\int_0^t P_n V_1(t')\,dt'\right\} \tag{VI.6}$$

still retains its unitarity (cf. Section 8 of paper II). It should be pointed out at this stage that the time development operator used by VOSLAMBER, 1969, is also unitary, but is significantly more complicated because it includes the effects of time ordering to one more order (third order) in the Dyson series. This does not necessarily entail better theoretical results since after the spherical average all the odd terms of the Dyson series do not contribute to the final results. Work which takes into account time ordering to all orders is in process and preliminary results for Lyman-α, which should reveal the strongest effects due to time ordering, show changes in the final line profile of only a few percent at the most.

VII. THE MULTIPOLE EXPANSION OF THE CLASSICAL INTERACTION POTENTIAL

Before evaluating the thermal average $\bar{\mathcal{F}}^{(1)}(t)$ we briefly consider the classical interaction potential $V_1(t)$ due to a single electron. If the perturber does not "penetrate" the

radiator. $V_1(t)$ is given by the well known multipole expansion

$$V_1(t) = e^2 \sum_{k=1}^{\infty} \frac{|\mathbf{R}|^k}{[r(t)]^{k+1}} \cdot P_k[\cos\theta(t)] \tag{VII.1}$$

where $|\mathbf{R}|$ is the distance of the orbital electron from the nucleus, $r(t)$ is the instantaneous distance of the perturbing electron, the P_k are Legendre polynomials and $\theta(t)$ is the instantaneous angle between $\mathbf{R}$ and $\mathbf{r}(t)$.

In most cases it is sufficient to consider only the dipole ($k = 1$) term. However, to account for some asymmetries of a line, it may be necessary to keep some of the higher multipole terms as well. In any case, one can show that this multipole expansion is terminated after some finite number of terms due to symmetries of the radiator.

To show this we specify the angular positions of $\mathbf{R}$ and $\mathbf{r}(t)$ by θ_1, φ_1 and θ_2, φ_2 respectively and we apply the spherical harmonic addition theorem (equation (4.6.7) of EDMONDS, 1960)

$$P_k(\cos\theta) = \sum_{p=-k}^{+k} (-1)^p C_p^k(\theta_1, \varphi_1) \cdot C_{-p}^k(\theta_2, \varphi_2) \tag{VII.2}$$

where

$$\cos\theta = \cos\theta_1 \cos\theta_2 + \sin\theta_1 \sin\theta_2 \cos(\varphi_1 - \varphi_2). \tag{VII.3}$$

We may simplify the mathematics without loosing generality by choosing a coordinate system in which $\varphi_2 = 0$. Using the relation

$$C_{-p}^k(\theta_2, \varphi_2 = 0) = (-1)^p \cdot C_p^k(\theta_2, \varphi_2 = 0) \tag{VII.4}$$

one then obtains

$$\begin{aligned} P_k(\cos\theta) = {} & C_0^k(\theta_1, \varphi_1) C_0^k(\theta_2) \\ & + \sum_{p=1}^{k} (-1)^p C_p^k(\theta_2, \varphi_2 = 0)[C_{-p}^k(\theta_1, \varphi_1) + (-1)^p C_p^k(\theta_1, \varphi_1)] \end{aligned} \tag{VII.5}$$

which gives for the interaction potential

$$\begin{aligned} V_1(t) = {} & e^2 \sum_{k=1}^{\infty} \frac{|\mathbf{R}|^k}{[r(t)]^{k+1}} \\ & \times \left[C_0^k \cdot P_k(\cos\theta_2(t)) + \sum_{p=1}^{k} \sqrt{\left(\frac{(k-p)!}{(k+p)!}\right)} P_k^p(\cos\theta_2(t)) \{C_{-p}^k + (-1)^p C_p^k\} \right]. \end{aligned} \tag{VII.6}$$

The dipole case ($k = 1$) gives the well known result

$$\begin{aligned} V_d(t) &= \frac{e^2|\mathbf{R}|}{r^2(t)} \left[C_0^1 \cos\theta_2(t) + \frac{1}{\sqrt{2}} \{C_{-1}^1 - C_1^1\} \sin\theta_2(t) \right] \\ &= \frac{e^2}{r^2(t)} [\mathbf{Z} \cdot \cos\theta_2(t) + \mathbf{X} \sin\theta_2(t)]. \end{aligned} \tag{VII.7}$$

The y-component vanished because $\varphi_2 = 0$. Similarly one can write down the higher order multipole terms. The necessary matrix elements of C_p^k are given by

$$\langle l'm'|C_p^k|lm\rangle = (-1)^{m'}\sqrt{[(2l'+1)(2l+1)]}\begin{pmatrix} l' & k & l \\ -m' & p & m\end{pmatrix}\begin{pmatrix} l' & k & l \\ 0 & 0 & 0\end{pmatrix}. \tag{VII.8}$$

From the last $3j$-symbol we see that these matrix elements exist only if l, k, l' satisfy the triangle condition and their sum is an even integer. Therefore it turns out that, within the no-quenching assumption where one needs the matrix elements of $P_n V_1(t)$, only a finite number of multiple terms exist. The summation index k in equation (VII.6) has to obey the condition

$$1 \leq k \leq 2(n-1). \tag{VII.9}$$

As an example we see that a calculation of the upper state interaction of Lyman-α requires only the dipole and quadrupole terms. This condition also illustrates the well known fact that there is no ground state interaction for the Lyman series.

VIII. THE SPHERICAL AVERAGE OF THE TIME DEVELOPMENT OPERATOR $\mathscr{U}_1(t)$

In our evaluation of the thermal average $\bar{\mathscr{F}}^{(1)}(t)$, defined in equation (VI.3), we first perform the spherical average represented by the integral over the Euler angles Ω, because it greatly simplifies the remaining integrals over t_0, ρ and v. This is due to the spherical symmetry of the time development operator $U_1(t)$ defined in equation (VI.6). It should be noted that this symmetry was achieved by dropping the ion field exponentials in equation (VI.4), thus replacing $\tilde{V}_1(t)$ by $V_1(t)$. We will perform this average by means of a rotation technique used by COOPER, 1967, and BARANGER, 1958, for S-matrices. Although we are working with the more general time development operators $U_1(t)$ or $\mathscr{U}_1(t)$, the rotation technique is the same.

In terms of the collision variables ρ, v, t_0 and Ω, the dipole interaction between the radiator and a perturber is given by

$$V_d(t) = e^2\mathbf{R}[\boldsymbol{\rho} + \mathbf{v}(t+t_0)]/[\rho^2 + v^2(t+t_0)^2]^{3/2} \tag{VIII.1}$$

(see the appendix of paper II). The three Euler angles denoted by Ω describe the orientation of the collision frame relative to the atomic frame. It is therefore convenient to perform a rotation of the atomic axis through the angles Ω in such a way that $\mathbf{R}$ points in the same direction as $\boldsymbol{\rho}$ and the x axis of the rotated atomic frame points in the same direction as $\mathbf{v}$. In this rotated frame, the interaction potential takes the form

$$V_c(t) = e^2[Z\rho + Xv(t+t_0)]/[\rho^2 + v^2(t+t_0)^2]^{3/2}. \tag{VIII.2}$$

This rotation transforms the time development operator U_1 into a new operator U_{1c}, where U_1 and U_{1c} are related to one another by

$$U_1 = \mathscr{D}^{-1}(\Omega)U_{1c}\mathscr{D}(\Omega) \tag{VIII.3}$$

where $\mathscr{D}(\Omega)$ is a rotation operator (see Chapter 4 of EDMONDS, 1960). The time development operator in the rotated frame, U_{1c}, is given by

$$U_{1c} = \exp\left\{-\frac{i}{\hbar}\int_0^t P_n V_c(t')\,dt'\right\}. \tag{VIII.4}$$

To make the form of U_{1c} more explicit, we perform the integral over t' and we obtain

$$U_{1c} = \exp\left\{-\frac{i}{\hbar}\frac{e^2}{\rho v}[P_n Z A(t, t_0, \rho, v) - P_n X B(t, t_0, \rho, v)\right\} \tag{VIII.5}$$

where

$$A(t, t_0, \rho, v) = \frac{(v/\rho)(t_0+t)}{\sqrt{[1+(v/\rho)^2(t_0+t)^2]}} - \frac{(vt_0/\rho)}{\sqrt{[1+(vt_0/\rho)^2]}} \tag{VIII.6}$$

and

$$B(t, t_0, \rho, v) = \frac{1}{\sqrt{[1+(v/\rho)^2(t_0+t)^2]}} - \frac{1}{\sqrt{[1+(vt_0/\rho)^2]}}. \tag{VIII.7}$$

Substituting equation (VIII.3) into equation (VI.3) we see that the integral over Ω in equation (VI.3) involves only the matrix elements of four rotation operators. Since it is convenient to use spherical states $|nlm\rangle$ when taking matrix elements of $\mathscr{D}(\Omega)$, we make use of the unitary transformation from parabolic to spherical states discussed by HUGHES, 1967.

$$|nqm\rangle = \sum_{lm'} |nlm'\rangle\langle nlm'|nqm\rangle$$

$$\langle nlm'|nqm\rangle = \delta_{mm'}(-1)^{1/2(1+m-q-n)}\sqrt{(2l+1)}\begin{pmatrix} \frac{n-1}{2} & \frac{n-1}{2} & l \\ \frac{m-q}{2} & \frac{m+q}{2} & -m \end{pmatrix} \tag{VIII.8}$$

using $3j$-symbols and the definitions in the equations (V.4) and (V.5). (An error in the phase factor has been pointed out by Pfennig, private communication.) Noting that $\mathscr{D}(\Omega)$ is diagonal in the angular momentum l, the Ω integral in equation (VI.3) may now be written

$$\int \langle n'q_b'm_b'; nq_bm_b|\mathscr{U}_1(t)|n'q_a'm_a'; nq_am_a\rangle \, d\Omega$$

$$= \sum\int d\Omega[\langle n'q_a'm_a'|n'l_a'm_a'\rangle \mathscr{D}^{(l_a')-1}_{m_a'm_c'}\langle n'l_a'm_c'|U_{1c}^{\dagger}|n'l_b'm_d'\rangle \tag{VIII.9}$$

$$\mathscr{D}^{(l_b')}_{m_d'm_b'}\langle n'l_b'm_b'|n'q_b'm_b'\rangle][\langle nq_bm_b|nl_bm_b\rangle$$

$$\mathscr{D}^{(l_b)-1}_{m_bm_d}\langle nl_bm_d|U_{1c}|nl_am_c\rangle\mathscr{D}^{(l_a)}_{m_cm_a}\langle nl_am_a|nq_am_a\rangle]$$

where the summation Σ denotes sums over l_a, l_a', l_b, l_b', m_c, m_c', m_d and m_d'. The Ω dependence of the integrand in equation (VIII.9) is contained entirely in the four rotation operators $\mathscr{D}(\Omega)$. Using equations (4.3.2) and (4.6.1) of EDMONDS, 1960, we obtain the identity

$$\int \mathscr{D}^{(l_a')-1}_{m_a'm_c'}\mathscr{D}^{(l_b')}_{m_d'm_b'}\mathscr{D}^{(l_b)-1}_{m_bm_d}\mathscr{D}^{(l_a)}_{m_cm_a} \, d\Omega = 8\pi^2 \sum_{L,M,M'} (-1)^{m_c'-m_a'+m_d-m_b+M-M'}(2L+1)$$

$$\times \begin{pmatrix} l_a' & l_a & L \\ -m_c' & m_c & M' \end{pmatrix}\begin{pmatrix} l_a' & l_a & L \\ -m_a' & m_a & M \end{pmatrix}\begin{pmatrix} l_b' & l_b & L \\ -m_d' & m_d & M' \end{pmatrix}\begin{pmatrix} l_b' & l_b & L \\ -m_b' & m_b & M \end{pmatrix}. \tag{VIII.10}$$

Hence equation (VIII.9) becomes

$$\int \langle n'q'_b m'_b; nq_b m_b|\mathscr{U}_1(t)|n'q'_a m'_a; nq_a m_a\rangle \, d\Omega = \sum \langle n'q'_a m'_a|n'l'_a m'_a\rangle\langle n'l'_b m'_b|n'q'_b m'_b\rangle$$

$$\times \langle nq_b m_b|nl_b m_b\rangle\langle nl_a m_a|nq_a m_a\rangle 8\pi^2 \sum_{L,M,M'} (-1)^{m'_c - m'_a + m_a - m_b + M - M'}(2L+1)$$

$$\times \begin{pmatrix} l'_a & l_a & L \\ -m'_c & m_c & M' \end{pmatrix}\begin{pmatrix} l'_a & l_a & L \\ -m'_a & m_a & M \end{pmatrix}\begin{pmatrix} l'_b & l_b & L \\ -m'_d & m_d & M' \end{pmatrix}\begin{pmatrix} l'_b & l_b & L \\ -m'_b & m_b & M \end{pmatrix}$$

$$\times \langle n'l'_b m'_d; nl_b m_d|\mathscr{U}_{1c}(t)|n'l'_a m'_c; nl_a m_c\rangle. \tag{VIII.11}$$

This result is spherically symmetric; that is, any further rotations of the atomic coordinate system leave this expression unchanged. One may verify this rotational invariance by rotating U_{1c} through some arbitrary angle Ω' so that $U_{1c} = \mathscr{D}^{-1}(\Omega')U'_{1c}\mathscr{D}(\Omega')$. Taking matrix elements of the new rotation operators and making use of the orthogonality properties of the $3j$-symbols one sees that the right hand side of equation (VIII.11) did not change. Since we are free to perform further rotations on U_{1c} without altering equation (VIII.11), it is convenient to rotate the X–Y plane through an angle $\varepsilon = \text{arctg}\,(B/A)$ where A and B are given by equations (VIII.6) and (VIII.7). This rotation transforms U_{1c} into an operator $\bar{U}_1$ given by

$$\bar{U}_1 = \exp\left\{-\frac{i}{\hbar}e^2 P_n Z g(t, t_0, \rho, v)\right\} \tag{VIII.12}$$

where

$$g(t, t_0, \rho, v) = \frac{1}{\rho v}\sqrt{(A^2 + B^2)} = \frac{\sqrt{2}}{\rho v}\left[1 - \frac{1 + (v/\rho)^2 t_0(t_0 + t)}{\sqrt{[1 + (v/\rho)^2(t_0 + t)^2]}\sqrt{[1 + (vt_0/\rho)^2]}}\right]^{1/2}. \tag{VIII.13}$$

The operator $\bar{U}_1$ has the important property that it is diagonal in parabolic states (because it contains only $P_n Z$). Hence a typical matrix element of U_1 is given by

$$\langle nqm|\bar{U}_1(t)|nqm\rangle = \exp\left\{-i\frac{3}{2}nq\frac{\hbar}{m}g(t, t_0, \rho, v)\right\}. \tag{VIII.14}$$

We also realize that one and the same rotation through the angle $\varepsilon = \text{arctg}\,(B/A)$ diagonalizes simultaneously both time development operators acting on initial and final states respectively. As a result a typical matrix element of the corresponding tetradic operator $\bar{\mathscr{U}}_1(t)$ is given by

$$\langle n'q'm'; nqm|\bar{\mathscr{U}}_1(t)|n'q'm'; nqm\rangle = \exp\left\{-i\frac{3}{2}(nq - n'q')\frac{\hbar}{m}g(t, t_0, \rho, v)\right\}. \tag{VIII.15}$$

Substituting this identity into equation (VIII.11) the spherical average of the time development operator $\mathscr{U}_1(t)$ finally becomes

$$\int \langle n'q_b'm_b'; nq_bm_b|\mathscr{U}_1(t)|n'q_a'm_a'; nq_am_a\rangle \,\mathrm{d}\Omega = \sum \langle n'q_a'm_a'|n'l_a'm_a'\rangle\langle n'l_a'm_c'|n'q_c'm_c'\rangle$$
$$\times\langle n'q_c'm_c'|n'l_b'm_c'\rangle\langle n'l_b'm_b'|n'q_b'm_b'\rangle\langle nq_am_a|nl_am_a\rangle\langle nl_am_c|nq_cm_c\rangle$$
$$\times\langle nq_cm_c|nl_bm_c\rangle\langle nl_bm_b|nq_bm_b\rangle 8\pi^2(-1)^{-m_a-m_b}(2L+1)$$
$$\times\begin{pmatrix} l_a' & l_a & L \\ -m_c' & m_c & M'\end{pmatrix}\begin{pmatrix} l_a' & l_a & L \\ -m_a' & m_a & M\end{pmatrix}\begin{pmatrix} l_b' & l_b & L \\ -m_c' & m_c & M'\end{pmatrix}\begin{pmatrix} l_b' & l_b & L \\ -m_b' & m_b & M\end{pmatrix}$$
$$\exp\left\{-i\frac{3}{2}(nq_c-n'q_c')\frac{\hbar}{m}g(t,t_0,\rho,v)\right\} \tag{VIII.16}$$

where the unitary transformations are given by equation (VIII.8). This result greatly simplifies if there is no lower state interaction (e.g. Lyman lines), in which case one obtains

$$\int \langle nq_bm_b|U_1(t)|nq_am_a\rangle \,\mathrm{d}\Omega = \sum \langle nq_bm_b|nl_am_a\rangle\langle nl_am_a|nq_am_a\rangle\delta_{m_am_b}[\langle nl_am_c|nq_cm_c\rangle]^2$$
$$\times\frac{8\pi^2}{2l_a+1}\exp\left\{-i\frac{3}{2}nq_c\frac{\hbar}{m}g(t,t_0,\rho,v)\right\}. \tag{VIII.17}$$

This simplified relation may also be used for the higher series members of the Balmer, Paschen etc. series where lower state interactions contribute only a negligible amount of broadening to the final line profile.

IX. EVALUATION OF THE THERMAL AVERAGE $\bar{\mathscr{F}}^{(1)}(t)$ FOR HYDROGEN

Having performed the spherical average over the Euler angles Ω we can rewrite equation (VI.3) in the form

$$\langle n'q_b'm_b'; nq_bm_b|\bar{\mathscr{F}}^{(1)}(t)|n'q_a'm_a'; nq_am_a\rangle = (-1)^{-m_a-m_b}\sum(2L-1)\langle n'q_a'm_a'|n'l_a'm_a'\rangle$$
$$\times\langle n'l_a'm_c'|n'q_c'm_c'\rangle\langle n'q_c'm_c'|n'l_b'm_c'\rangle\langle n'l_b'm_b'|n'q_b'm_b'\rangle\langle nq_am_a|nl_am_a\rangle\langle nl_am_c|nq_cm_c\rangle$$
$$\times\langle nq_cm_c|nl_bm_c\rangle\langle nl_bm_b|nq_bm_b\rangle\begin{pmatrix} l_a' & l_a & L \\ -m_c' & m_c & M'\end{pmatrix}\begin{pmatrix} l_a' & l_a & L \\ -m_a' & m_a & M\end{pmatrix}\begin{pmatrix} l_b' & l_b & L \\ -m_c' & m_c & M'\end{pmatrix}$$
$$\times\begin{pmatrix} l_b' & l_b & L \\ -m_b' & m_b & M\end{pmatrix}\bar{F}(t,n,q_c,n',q_c') \tag{IX.1}$$

where

$$\bar{F}(t,n,q_c,n',q_c') = 2\pi n_e\int \mathrm{d}v\, vf(v)\int \mathrm{d}\rho\,\rho\int \mathrm{d}t_0\Phi(t,t_0,\rho,v) \tag{IX.2}$$

and

$$\Phi(t,t_0,\rho,v) = \exp\left\{-i\frac{3}{2}(nq_c-n'q_c')\frac{\hbar}{m}g(t,t_0,\rho,v)\right\}-1. \tag{IX.3}$$

Thus, the problem is now reduced to evaluating $\bar{F}(t)$, which will be done in this section. It is interesting to note the similarity between equations (VIII.13) and (IX.2) and the Ψ-function of ANDERSON and TALMAN, 1955, which is the crucial function in their classical adiabatic theory.

We first realize that due to the symmetry of the line profile we only have to evaluate the real part of $\Phi(t, t_0, \rho, v)$; that is, for every positive value of $(nq_c - n'q_c')$ there will be the corresponding negative value. Hence we are left with

$$\Phi(t, t_0, \rho, v) = \cos\left\{\frac{3}{2}(nq_c - n'q_c')\frac{\hbar}{m}g(t, t_0, \rho, v)\right\} - 1. \tag{IX.4}$$

In performing the integrals over ρ and t_0 in equation (IX.2) we account for shielding by setting the interaction potential V and hence also Φ equal to zero whenever the distance of the perturbing electron is larger than the Debye length D. We also introduce a strong collision cutoff $\rho_{\min}$. In principle we can let the impact parameter go to zero because the functions Φ and $F(t)$ do not diverge for small impact parameters as they do in some second order theories. However, for numerical purposes this would result in very large computer times due to the growing fluctuations in the integral. For this reason we will choose ρ_{min} to be small enough so that when we are interested in large frequency perturbations $\Delta\omega$ where perturbers at small impact parameters are quasistatic, the rest of the integral from 0 to $\rho_{\min}$ may then be replaced by the static limit. In the dipole approximation this gives rise to the well known Holtsmark $\Delta\lambda^{-5/2}$-wing (see also Section X). According to the validity conditions of the classical path theories (see paper I) the minimum impact parameter $\rho_{\min}$ will be of the order of

$$\rho_0 = \lambda\!\!\!^{-} + n^2 a_0 \tag{IX.5}$$

where $\lambda\!\!\!^{-}$ is the De Broglie wavelength.

We now concentrate our attention on the integral

$$G(t, \rho, v) = \int \mathrm{d}t_0\, \Phi(t, t_0, \rho, v). \tag{IX.6}$$

For convenience we consider the collision sphere as shown in Fig. 1. The perturbing electron moves along the classical straight line trajectory L and we are interested in the interaction from some time t_0 to some time $t_0 + t$. Due to the Debye cutoff the t_0-integral extends from $-T$ to $+T$ where

$$T = \frac{1}{v}\sqrt{(D^2 - \rho^2)} \tag{IX.7}$$

and the interaction potential vanishes if the electron is outside the sphere of radius D. The corresponding time integration limit τ due to the strong collision cutoff $\rho_{\min}$ is given by

$$\tau = \frac{1}{v}\sqrt{(\rho_0^2 - \rho^2)}. \tag{IX.8}$$

Based on this model of the collision sphere we split the integral G into two parts

$$G(t, \rho, v) = U(\rho > \rho_0) \cdot G_a(t, \rho, v) + U(\rho_0 > \rho) \cdot G_b(t, \rho, v) \tag{IX.9}$$

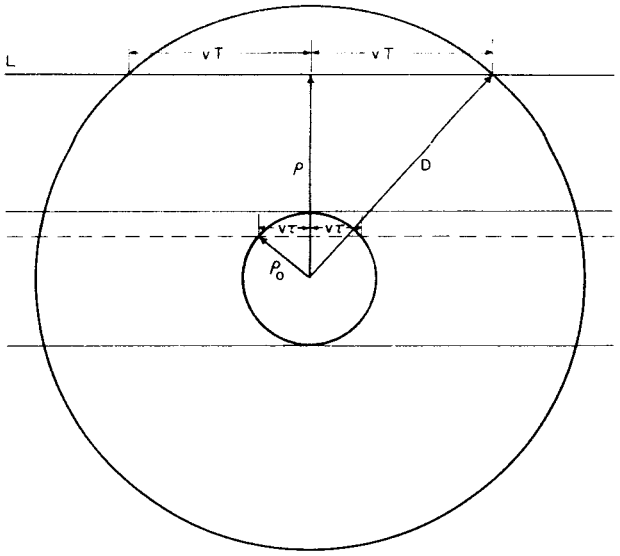

FIG. 1. Schematic picture of the collision sphere showing the Debye sphere, a strong collision sphere and a straight line classical path trajectory.

where the step function U is defined to be

$$U(a > b) = \begin{cases} 1 & \text{if } a \geq b \\ 0 & \text{if } a < b \end{cases} \tag{IX.10}$$

In order to evaluate $G_a(t, \rho, v)$ we have to distinguish the following four cases depending on whether the initial and final times of interaction are inside or outside the sphere.

Case 1: $-T < t_0; t_0 + t < T$

$$g_1(t, t_0, \rho, v) = \frac{\sqrt{2}}{\rho \cdot v}\left[1 - \frac{1 + \frac{v^2}{\rho^2} t_0(t_0 + t)}{\sqrt{\left\{\left[1 + \frac{v^2}{\rho^2}(t_0 + t)^2\right]\left[1 + \frac{v^2}{\rho^2} t_0^2\right]\right\}}}\right]^{1/2}. \tag{IX.11a}$$

This is the same general expression as given in equation (VIII.13).

Case 2: $-T < t_0; T < t_0 + t$

$$g_2(t, t_0, \rho, v) = \frac{\sqrt{2}}{\rho \cdot v}\left[1 - \frac{\frac{\rho}{D} + \frac{v}{\rho} t_0 \sqrt{\left(1 - \frac{\rho^2}{D^2}\right)}}{\sqrt{\left(1 + \frac{v^2}{\rho^2} t_0^2\right)}}\right]^{1/2}. \tag{IX.11b}$$

Case 3: $t_0 < -T; t_0 + t < T$

$$g_3(t, t_0, \rho, v) = \frac{\sqrt{2}}{\rho \cdot v}\left[1 - \frac{\frac{\rho}{D} - \frac{v}{\rho}(t_0 + t) \sqrt{\left(1 - \frac{\rho^2}{D^2}\right)}}{\sqrt{\left[1 + \frac{v^2}{\rho^2}(t_0 + t)^2\right]}}\right]^{1/2}. \tag{IX.11c}$$

Case 4: $t_0 < -T;\ T < t_0+t$

$$g_4(t, t_0, \rho, v) = \frac{2}{\rho v}\sqrt{\left(1-\frac{\rho^2}{D^2}\right)}. \tag{IX.11d}$$

After defining

$$\Phi_k(t, t_0, \rho, v) = \cos\left\{\frac{3}{2}(nq_c - n'q_c')\frac{\hbar}{m}g_k(t, t_0, \rho, v)\right\} - 1 \tag{IX.12}$$

the integral G_a is given by

$$G_a(t, \rho, v) = U(2T > t)\left\{\int_{-T}^{T-t}\Phi_1\,dt_0 + \int_{T-t}^{T}\Phi_2\,dt_0 + \int_{-T-t}^{-T}\Phi_3\,dt_0\right\}$$
$$+ U(t > 2T)\left\{\int_{-T}^{T}\Phi_2\,dt_0 + \int_{-T-t}^{T-t}\Phi_3\,dt_0 + \int_{T-t}^{-T}\Phi_4\,dt_0\right\} \tag{IX.13}$$

where we have separated the cases where the time of interaction is longer or shorter than the time $2T$ required to cross the collision sphere.

In a similar manner we evaluate G_b distinguishing between the following cases:

Case 1: $-T < t_0;\ t_0+t < -\tau$ or $\tau < t_0;\ t_0+t < \mathrm{T}$

$$g(t, t_0, \rho, v) = g_1(t, t_0, \rho, v). \tag{IX.14a}$$

Case 2: $\tau < t_0 < T;\ T < t_0+t$

$$g(t, t_0, \rho, v) = g_2(t, t_0, \rho, v). \tag{IX.14b}$$

Case 3: $t_0 < -T;\ -T < t_0+t < -\tau$

$$g(t, t_0, \rho, v) = g_3(t, t_0, \rho, v). \tag{IX.14c}$$

Collisions which enter the strong collision sphere are neglected because of the strong oscillations. This yields

$$G_b(t, \rho, v) = U(T-\tau > t)\left\{\int_{-T}^{-\tau-t}\Phi_1\,dt_0 + \int_{\tau}^{T-t}\Phi_1\,dt_0 + \int_{T-t}^{T}\Phi_2\,dt_0 + \int_{-T-t}^{-T}\Phi_3\,dt_0\right\}$$
$$+ U(t > T-\tau)\left\{\int_{\tau}^{T}\Phi_2\,dt_0 + \int_{-T-t}^{-\tau-t}\Phi_3\,dt_0\right\} \tag{IX.15}$$

where again interaction times longer or shorter than $(T-\tau)$ have been separated. In the expressions for G_a and G_b we realize after a change of variables that the corresponding integrals over Φ_2 and Φ_3 are identical. From the equations (IX.11a) and (IX.12) it is also clear that Φ_1 is a symmetric function in $z = t_0+t/2$. Performing the Φ_4-integral one finally

obtains

$$\tfrac{1}{2}\cdot G_a(t,\rho,v) = U(2T>t)\left\{\int_{-t/2}^{T-t}\Phi_1\,dt_0+\int_{T-t}^{T}\Phi_2\,dt_0\right\} + U(t>2T)\left\{\int_{-T}^{+T}\Phi_2\,dt_0+\left(\frac{t}{2}-T\right)\cdot\Phi_4\right\} \tag{IX.16a}$$

and

$$\tfrac{1}{2}\cdot G_b(t,\rho,v) = U(T-\tau>t)\left\{\int_{\tau}^{T-t}\Phi_1\,dt_0+\int_{T-t}^{T}\Phi_2\,dt_0\right\}+U(t>T-\tau)\left\{\int_{\tau}^{T}\Phi_2\,dt_0\right\}. \tag{IX.16b}$$

We now introduce the following dimensionless variables

$$\begin{aligned} x &= \frac{\rho}{D} \quad\text{and}\quad x_0=\frac{\rho_0}{D} \quad\text{with}\quad D=\sqrt{\left(\frac{kT}{4\pi n_e e^2}\right)},\\ s &= \tilde{\omega}_p t \quad\text{with}\quad \tilde{\omega}_p=\sqrt{2}\cdot\omega_p=\sqrt{\left(\frac{8\pi n_e e^2}{m}\right)},\\ y &= t_0/T\\ u &= \frac{v}{v_{\mathrm{av}}} \quad\text{with}\quad v_{\mathrm{av}}=\sqrt{\left(\frac{2kT}{m}\right)} \end{aligned} \tag{IX.17}$$

and the following abbreviations

$$\begin{aligned} R &= \frac{t}{T}=\frac{u\cdot s}{\sqrt{(1-x^2)}}\\ P &= \frac{\tau}{T}=\frac{\sqrt{(x_0^2-x^2)}}{\sqrt{(1-x^2)}}. \end{aligned} \tag{IX.18}$$

With these definitions the preceding relations can be rewritten as

$$\begin{aligned} g_1(s,y,x,u) &= \frac{\sqrt{2}}{xu}\cdot\left[1-\frac{x^2+(1-x^2)y(y+R)}{\sqrt{\{[x^2+(1-x^2)y^2][x^2+(1-x^2)(y+R)^2]\}}}\right]^{1/2}\\ g_2(s,y,x,u) &= \frac{\sqrt{2}}{xu}\cdot\left[1-\frac{x^2+y(1-x^2)}{\sqrt{[x^2+y^2(1-x^2)]}}\right]^{1/2}\\ g_4(s,y,x,u) &= \frac{2}{xu}\cdot\sqrt{(1-x^2)} \end{aligned} \tag{IX.19}$$

and

$$\Phi_k(s,y,x,u) = \cos\{C\cdot g_k(s,y,x,u)\}-1 \tag{IX.20}$$

where

$$C = C_1 \cdot C_2 \tag{IX.21a}$$

and

$$C_1 = \tfrac{3}{2}(nq_c - n'q_c') \tag{IX.21b}$$

$$C_2 = \frac{\hbar}{m \cdot D \cdot v_{av}} = \frac{\hbar\tilde{\omega}_p}{2kT} = 0.03043\sqrt{\left(\frac{Ncm^3}{10^{18}}\right)} \cdot \frac{10^4 K}{T}.$$

Similarly we have for the integrals over t_0

$$G_a(s, x, u) = U(2 > R)\left\{\int_{-R/2}^{1-R} \Phi_1 \, dy + \int_{1-R}^{1} \Phi_2 \, dy\right\} + U(R > 2)\left\{\int_{-1}^{+1} \Phi_2 \, dy + \left(\frac{R}{2} - 1\right)\Phi_4\right\} \tag{IX.22a}$$

and

$$G_b(s, x, u) = U(1 > R+P)\left\{\int_{P}^{1-R} \Phi_1 \, dy + \int_{1-R}^{1} \Phi_2 \, dy\right\} + U(R+P > 1)\left\{\int_{P}^{1} \Phi_2 \, dy\right\} \tag{IX.22b}$$

which leads to the thermal average

$$\bar{F}(s, n_e, T) = 2\pi n_e D^3 \int_0^\infty du \frac{4}{\sqrt{\pi}} u^2 \cdot e^{-u^2} \int_0^1 dx \, x\sqrt{(1-x^2)2} \cdot G(s, x, u) \tag{IX.23}$$

with

$$G(s, x, u) = U(x > x_0) \cdot G_a(s, x, u) + U(x_0 > x) \cdot G_b(s, x, u). \tag{IX.24}$$

These integrals have been evaluated numerically.

Before we discuss the methods for obtaining the Fourier transform of $\bar{F}(t)$ and the actual intensity profile, it is useful to derive the small and large time limit of $\bar{F}(t)$. The small time limit is determined by the integrals over Φ_1 and gives the asymptote of the thermal average for the static wing. The large time limit depends only on the Φ_4 integrals and yields the thermal average as required by the impact theory.

In the small time limit Φ_1 reduces to the form

$$\Phi_1(t, r)_{t\to 0} = \cos\left\{\frac{3}{2}(nq_c - n'q_c')\frac{\hbar}{m}\frac{t}{r^2}\right\} - 1 \tag{IX.25}$$

where

$$r = \sqrt{(\rho^2 + v^2 t_0^2)}. \tag{IX.26}$$

This expression depends only on the instantaneous distance r as expected in the static limit and the thermal average is therefore obtained immediately by the integral over r

$$\bar{F}(t)_{t\to 0} = 4\pi n_e \int_0^{r_c} r^2 \Phi_1(t, r)_{t\to 0} \, dr. \tag{IX.27}$$

In the small time limit where

$$\frac{3}{2}(nq_c - n'q_c')\frac{\hbar}{m}\cdot\frac{t}{r_c^2} \to 0$$

we can then perform the integral with the result

$$\bar{F}(t)_{t\to 0} = -\frac{2}{3}n_e\left[3\pi(nq_c - n'q_c')\frac{\hbar}{m}t\right]^{3/2} \tag{IX.28}$$

For the limit of large times of interaction we have to solve the integral

$$\bar{F}(t)_{t\to\infty} = 2\pi n_e\int_0^\infty \mathrm{d}v\, vf(v)\int_{\rho_0}^D \mathrm{d}\rho\, \rho t\cdot\Phi_4. \tag{IX.29}$$

For simplicity we set ρ_0 equal to zero (for $\rho_0 \neq 0$ see the Appendix). After a change of variables and a partial integration the integral can be rewritten as

$$\bar{F}(t)_{t\to\infty} = -2\pi n_e t D^2 v_{\mathrm{av}}\int_0^\infty \mathrm{d}u\frac{4}{\sqrt{\pi}}u^2 e^{-u^2}C\int_0^\infty \frac{\sin[(2C/u)z]}{1+z^2}\,\mathrm{d}z. \tag{IX.30}$$

The z-integral is known as Raabe's integral (see p. 144 of BATEMAN, 1953) and can be expressed in terms of exponential integrals. Furthermore, from equation (IX.21) we realize that for most practical situations $C \ll 1$. Keeping only the leading term in C we have

$$\begin{aligned}\bar{F}(t)_{t\to\infty} &= -4\sqrt{(\pi)}C^2 n_e D^2 v_{\mathrm{av}} t[B - \ln(4C^2)] \\ &= -\left(\frac{3}{2}(nq_c - n'q_c')\frac{\hbar}{m}\right)^2 n_e t\sqrt{\left(\frac{8\pi m}{kT}\right)}[B - \ln(4C^2)]\end{aligned} \tag{IX.31}$$

where

$$4C^2 = \frac{2\pi n_e}{m}\left(\frac{3(nq_c - n'q_c')\hbar e}{kT}\right)^2 \quad \text{and} \quad B = 0.27. \tag{IX.32}$$

The large time limit of the thermal average in equation (IX.31) is required for the calculation of the line center and all modern impact theories give the same result except for the additive constant B whose value depends on the particular cutoff procedure applied. The Appendix gives a summary of the different constants obtained in the literature which vary considerably. To what extent this uncertainty shows up in the final line profile depends on the value of the constant C. The influence will be small if $\ln(4C^2)$ is considerably larger than the uncertainty in the additive constant B. Furthermore, the large time limit of the thermal average affects primarily the center of the line profile and its contribution vanishes when moving into the line wings.

Finally we show numerical results for $\bar{F}(t)$ as obtained by means of a program described by VIDAL, 1970. Most of the calculations shown in this paper have been performed for the following electron density and temperature parameters. These parameters correspond to experiments which, as stated already in the introduction, have revealed the largest

Case	n_e [cm^{-3}]	T_e[K]	Experiment
A	$8.4 \cdot 10^{16}$	12 200	BOLDT and COOPER, 1964 (cascade arc)
B	$3.6 \cdot 10^{17}$	20 400	ELTON and GRIEM, 1964 (T-shock tube)
C	$1.3 \cdot 10^{13}$	1850	VIDAL, 1964 (RF-discharge)

discrepancies between experiment and the modified impact theory. We will concentrate our attention on the high density case A and the low density case C, since case B is regarded as being less accurate because of lacking absolute intensity calibrations.

Figures 2 and 3 show the normalized thermal average $\bar{F}/\bar{F}_0$ as a function of the dimensionless variable $s = \tilde{\omega}_p \cdot t$ for the cases A and C. Figure 3 shows the results for three different Stark components specified by the quantum numbers $n_k = nq_c - n'q_c'$. $\bar{F}_0$ is the small time limit according to equation (IX.28) whose Fourier transform leads to the static wing. The dashed lines are obtained with a lower cutoff $\rho_{\min} = \rho_0 = \hat{\lambda} + n^2 a_0$. It can be seen that for case C the dashed curves get closer to the static limit $\bar{F}_0$ than for case A. In order to obtain the thermal average $\bar{F}$ for the limit $\rho_{\min} \to 0$ the numerical

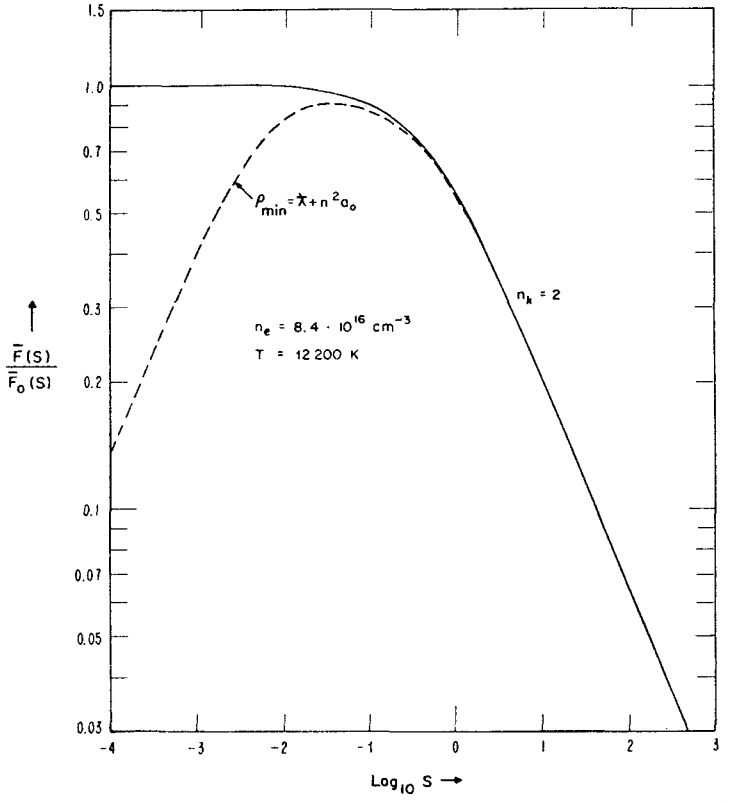

FIG. 2. The thermal average $\bar{F}$ of the time development operator normalized with respect to the static, small interaction time asymptote $\bar{F}_0$ as a function of the normalized time $s = \tilde{\omega}_p \cdot t$. The two curves are obtained with two different lower cutoff parameters in the ρ-integral. $\rho_{\min} = 0$ and $\rho_{\min} = \hat{\lambda} + n^2 a_0$.

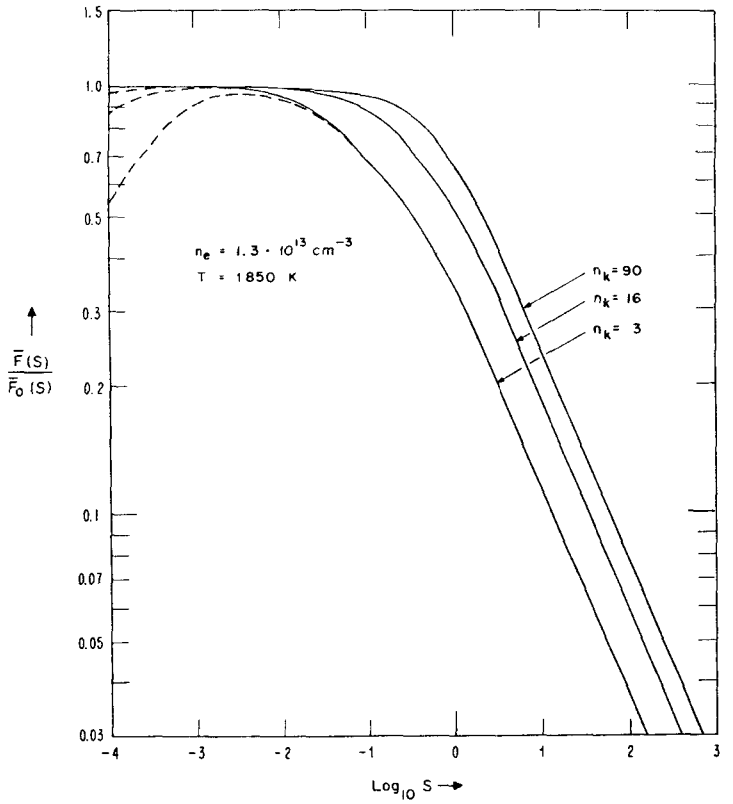

FIG. 3. The thermal average $\bar{F}$ of the time development operator normalized with respect to the static, small interaction time asymptote $\bar{F}_0$ as a function of the normalized time $s = \tilde{\omega}_p t$. The two sets of curves are obtained with two different lower cutoff parameters in the ρ-integral, $\rho_{min} = 0$ and $\rho_{min} = \lambda + n^2 a_0$. The three different curves in every set correspond to different Stark components characterized by the quantum number $n_k = nq - n'q'$.

calculations were finally performed with typically $\rho_{min} \simeq 0.01\rho_0$ so that $\bar{F}_{calc}$ and $\bar{F}_0$ differed less than about 0.1 per cent over at least one order of magnitude in s. For smaller values of s, where $\bar{F}_{calc}$ and $\bar{F}_0$ start to differ again, $\bar{F}_{calc}$ is then replaced by $\bar{F}_0$. In this manner we obtain the solid curves in Figs. 2 and 3 which are used in the following.

It should be noted that these curves are calculated on the basis of the dipole approximation. It is clear that for impact parameters $\rho \gtrsim n^2 a_0$ higher multipole terms have to be considered. Since the values s of interest are approximately given by $s \gtrsim \tilde{\omega}_p/\Delta\omega$, one expects higher multipole terms to be less important the closer $\bar{F}_{calc}$ gets to $\bar{F}_0$ for $\rho_{min} = n^2 a_0$. This is consistent with the experimental fact that in case A an asymmetry of the line has been observed which cannot be explained within the dipole approximation, while in case C no asymmetry has been observed.

For large s Figs. 2 and 3 show the transition to $\bar{F}_\infty$ as given in equation (IX.31), which forms the basis for the familiar impact theories.

X. THE FOURIER TRANSFORM OF THE THERMAL AVERAGE

Having calculated the thermal average $\bar{F}(t)$ we now focus our attention on the evaluation of its Fourier transform

$$i(\Delta\omega_R) = \frac{1}{\pi}\int_0^\infty \exp(i\Delta\omega_R s)\bar{F}(s)\,ds \tag{X.1}$$

as required by equation (V.17) (see also equation (IV.16)) where the dimensionless variable

$$\Delta\omega_R = (\Delta\omega - \Delta\omega_i \cdot \beta)/\tilde{\omega}_p \tag{X.2}$$

is the frequency separation from a particular Stark component (cf. equation (V.14)) for an ion field strength β in units of the plasma frequency $\tilde{\omega}_p$.

The thermal average $\bar{F}(s)$ does not immediately allow a straightforward Fourier transformation because for large s $\bar{F}(s)$ is proportional to s according to equation (IX.31), hence $i(\Delta\omega_R)$ diverges. This divergence is due to the fact that we neglected the finite lifetimes of the unperturbed states involved which naturally terminate the maximum time of interaction s. This may be taken care of by introducing a convergence factor $\exp(-\varepsilon s)$ which can be obtained by replacing the delta function in the power spectrum of equation (3) in paper I by a narrow Lorentzian line with a natural width ε (SMITH and HOOPER, 1967). In the final line profile, however, natural line broadening is always negligible with respect to Stark broadening which allows us to set ε to zero without affecting the shape of the profile. For this reason we will evaluate

$$i(\Delta\omega_R) = \lim_{\varepsilon\to 0}\frac{1}{\pi}\int_0^\infty e^{-\varepsilon s}e^{i\Delta\omega_R s}\bar{F}(s)\,ds \tag{X.3}$$

$\bar{F}(s)$ is known numerically and there are many ways to perform the Fourier transform. In order to find the most convenient method we notice that according to equations (IX.28) and (IX.31), $\bar{F}(s)$ has the following asymptotes

$$\begin{aligned} &\text{for} \quad s \to 0\colon \ \bar{F}_0(s) = p_1 s^{3/2} \\ &\text{and for} \quad s \to \infty\colon \ \bar{F}_\infty(s) = p_2 s, \end{aligned} \tag{X.4}$$

where

$$p_1 = -\tfrac{2}{3}n_e D^3(2\pi C)^{3/2} \tag{X.5}$$

and

$$p_2 = -4\sqrt{(\pi)}n_e D^3 C^2[B - \ln(4C^2)].$$

The transition from $\bar{F}_0$ to $\bar{F}_\infty$ is very smooth because the power in s changes only by $\frac{1}{2}$ over the entire range. It has been found that $\bar{F}(s)$ may be approximated by a function $G(s)$ whose Fourier transform can be given analytically and whose parameters may be determined by a least square fit. The function $G(s)$ can be given in terms of the series

$$G(s) = \sum_k G_k(s), \tag{X.6}$$

where the number of terms in the series depends on the required accuracy. As a first approximation equation (X.4) suggests

$$G_1(s) = \frac{a_1 s^2}{\sqrt{(s^2 + 2b_1 s)}} \tag{X.7}$$

with

$$a_1 = p_2 \tag{X.8}$$

and

$$b_1 = \tfrac{1}{2}(p_2/p_1)^2.$$

$G_1(s)$ has the small and large s behavior of $\bar{F}(s)$. It then turns out that

$$\begin{aligned} &\text{for } s \to 0 \quad \bar{F}(s) - G_1(s) = p_3 s^{5/2} \\ &\text{and for } s \to \infty \quad \bar{F}(s) - G_1(s) = p_4, \end{aligned} \tag{X.9}$$

where p_3 and p_4 now have to be determined numerically. Consequently we take $G_2(s)$ to be

$$G_2(s) = \frac{a_2 s^5}{(s^2 + 2b_2 s)^{5/2}}. \tag{X.10}$$

It then becomes apparent that $G_k(s)$ is given by

$$G_k(s) = \frac{a_k s^{3k-1}}{(s^2 + 2b_k s)^{2k-3/2}} \tag{X.11}$$

with

$$a_k = p_{2k} \quad \text{and} \quad b_k = \tfrac{1}{2}(p_{2k}/p_{2k-1})^{2/(4k-3)} \tag{X.12}$$

such that one obtains

$$\begin{aligned} &\text{for} \quad s \to 0: \quad G(s) = \sum_{k=1}^{\infty} p_{2k-1} s^{k+1/2} \\ &\text{and for} \quad s \to \infty: \quad G(s) = \sum_{k=1}^{\infty} p_{2k} \cdot s^{2-k}. \end{aligned} \tag{X.13}$$

In this manner the Fourier transform of any $G_k(s)$ can be expressed in terms of modified Bessel functions K_0 and K_1. For all situations calculated it was found that $G_1(s)$ and $G_2(s)$ were sufficient to keep the deviation $\bar{F}(s)$–$G(s)$ smaller than 1 per cent for all values of s. In some situations a fit better than 2 per cent was obtained with $G_1(s)$ alone. As a further advantage it should be noted that this method tends to suppress "noise" introduced by the numerical evaluation of $\bar{F}(s)$.

In the following we evaluate the Fourier transform $i(k, \Delta\omega_R)$ of any $G_k(s)$ as defined by

$$i(k, \Delta\omega_R) = \lim_{\varepsilon \to 0} \frac{1}{\pi} \int_0^{\infty} \mathrm{e}^{-\varepsilon s} \mathrm{e}^{i\Delta\omega_R s} G_k(s)\, \mathrm{d}s. \tag{X.14}$$

Their sum will then give us the desired Fourier transform $i(\Delta\omega_R)$. In particular we are interested in $i(k=1,\Delta\omega_R)$ and $i(k=2,\Delta\omega_R)$. We have

$$i_1(\Delta\omega_R) = i(k=1,\Delta\omega_R) = \lim_{\varepsilon\to 0}\frac{1}{\pi}\int_0^\infty e^{-\varepsilon s}e^{i\Delta\omega_R s}\frac{a_1 s^2}{\sqrt{(s^2+2b_1 s)}}\,ds$$

$$= a_1\lim_{\varepsilon\to 0}\frac{1}{\pi}\frac{d^2}{d\varepsilon^2}\int_0^\infty \frac{e^{-\varepsilon s}e^{i\Delta\omega_R s}}{\sqrt{(s^2+2b_1 s)}}\,ds$$

$$= a_1\lim_{\varepsilon\to 0}\frac{1}{\pi}\frac{d^2}{d\varepsilon^2}\{e^{b_1(\varepsilon-i\Delta\omega_R)}K_0[b_1(\varepsilon-i\Delta\omega_R)]\}. \tag{X.15}$$

Introducing

$$Z_1 = b_1\Delta\omega_R \tag{X.16}$$

one finally obtains

$$i_1(\Delta\omega_R) = a_1\cdot b_1^2\cdot e^{-iZ_1}\left\{iH_0^{(1)}(Z_1)+H_1^{(1)}(Z_1)\left[1-\frac{i}{2Z_1}\right]\right\}$$

$$= a_1\cdot b_1^2(\cos Z_1 - i\sin Z_1)$$

$$\times\left[\left(J_1(Z_1)-Y_0(Z_1)+\frac{Y_1(Z_1)}{2Z_1}\right)+i\left(J_0(Z_1)+Y_1(Z_1)-\frac{J_1(Z_1)}{2Z_1}\right)\right] \tag{X.17}$$

Here $H_0^{(1)}$ and $H_1^{(1)}$ are Hankel functions and J_0, J_1, Y_0 and Y_1 Bessel functions. These functions like all the other functions used in this paper are consistent with the definitions as given, for example, by the *NBS Handbook of Mathematical Functions* (ABRAMOWITZ, 1969). For large arguments Z_1 it is also useful to have the asymptotic expansion

$$i_1(\Delta\omega_R) = -\frac{3}{8}\frac{a_1\cdot b_1^2}{\sqrt{(\pi Z_1)}}\cdot\frac{1}{Z_1^2}\left\{1+i+\frac{5}{8Z_1}(1-i)-\frac{3\cdot 5\cdot 7}{2\cdot 8^2 Z_1^2}(1+i)\right.$$

$$\left.-\frac{9\cdot 25\cdot 7}{2\cdot 8^3 Z_1^3}(1-i)+\frac{9\cdot 25\cdot 49\cdot 11}{8^5 Z_1^4}(1+i)+--\cdots\right\}$$

$$= -\frac{3}{8}\sqrt{\left(\frac{2}{\pi}\right)}p_1\Delta\omega_R^{-5/2}\left\{1+i+\frac{5}{4}\left(\frac{p_1}{p_2}\right)^2\frac{(1-i)}{\Delta\omega_R}-\frac{105}{32}\left(\frac{p_1}{p_2}\right)^2\frac{(1+i)}{\Delta\omega_R^2}-++\cdots\right\}. \tag{X.18}$$

Using equation (X.5) for p_1 the latter relation gives us exactly the Holtsmark $\Delta\lambda^{-5/2}$ wing for all Stark components

$$i_H(\Delta\omega_R) = \pi n_e D^3 C^{3/2}\cdot\Delta\omega_R^{-5/2}. \tag{X19}$$

In a similar way one derives

$$i_2(\Delta\omega_R) = i(k=2,\Delta\omega_R) = \lim_{\varepsilon\to 0}\frac{1}{\pi}\int_0^\infty e^{-\varepsilon s}e^{i\Delta\omega_R s}\frac{a_2 s^5}{(s^2+2b_2 s)^{5/2}}\,ds$$

$$= -\frac{a_2}{3}\lim_{\varepsilon\to 0}\frac{1}{\pi}\frac{d^3}{d\varepsilon^3}\frac{d^2}{db_2^2}\int_0^\infty\frac{e^{-\varepsilon s}e^{i\Delta\omega_R s}}{\sqrt{(s^2+2b_2 s)}}\,ds. \tag{X.20}$$

With

$$Z_2 = b_2 \Delta\omega_R \tag{X.21}$$

one finally obtains

$$\begin{aligned} i_2(\Delta\omega_R) &= \frac{a_2 b_2}{6} \cdot e^{-iZ_2}\{H_0^{(1)}(Z_2)(i16Z_2^2 - 36Z_2 - i15) + H_1^{(1)}(Z_2)(16Z_2^2 + i28Z_2 - 3)\} \\ &= \frac{a_2 b_2}{6}(\cos Z_2 - i \sin Z_2) \\ &\quad \times \{[-36Z_2 J_0(Z_2) + J_1(Z_2)(16Z_2^2 - 3) - Y_0(Z_2)(16Z_2^2 - 15) - 28Z_2 Y_1(Z_2)] \\ &\quad + i[J_0(Z_2)(16Z_2^2 - 15) + 28Z_2 J_1(Z_2) - 36Z_2 Y_0(Z_2) + Y_1(Z_2)(16Z_2^2 - 3)]\}. \end{aligned} \tag{X.22}$$

The asymptotic expansion for large Z_2 is given by

$$i_2(\Delta\omega_R) = \frac{15}{64}\frac{a_2 b_2}{\sqrt{\pi}} Z_2^{-7/2}\left(1 - i - \frac{35}{8Z_2}(1+i) - \frac{35 \cdot 63}{128 Z_2^2}(1-i) + \cdots\right). \tag{X.23}$$

If one requires an even better fit of $G(s)$ to $\bar{F}(s)$ the general transform $i(k, \Delta\omega_R)$ as defined in equation (X.14) is given by

$$i(k, \Delta\omega_R) = \frac{4^{k-1}(2k-2)!}{(4k-4)!} a_k \lim_{\varepsilon \to 0} \frac{1}{\pi}(-1)^{k+1} \frac{d^{k+1}}{d^{k+1}\varepsilon} \frac{d^{2k-2}}{d^{2k-2} b_k}\{e^{b_k(\varepsilon - i\Delta\omega_R)} K_0[b_k(\varepsilon - i\Delta\omega_R)]\}. \tag{X.24}$$

Finally we want to show that this technique always gives the static wing according to equation (X.19) for large $\Delta\omega$. For this purpose one has to perform the Fourier transform of the small time limit of $G(s)$ as given in equation (X.13).

$$\begin{aligned} i_\infty(\Delta\omega_R) &= \lim_{\Delta\omega_R \to \infty} i(\Delta\omega_R) = \sum_{k=1}^{\infty} p_{2k-1} \lim_{\varepsilon \to 0} \frac{1}{\pi} \int_0^\infty e^{-\varepsilon s} e^{i\Delta\omega_R s} s^{k+1/2}\, ds \\ &= \frac{1}{\sqrt{\pi}} \sum_{k=1}^{\infty} \frac{(2k+1)!}{2^{2k+1} k!} p_{2k-1} \exp\left[i\frac{\pi}{2}\left(\frac{3}{2} + k\right)\right] \Delta\omega_R^{-(k+3/2)} \\ &= \frac{3}{8}\sqrt{\left(\frac{2}{\pi}\right)} \frac{1}{\Delta\omega_R^{5/2}} \left\{-p_1(1+i) + \frac{5}{2}\frac{p_3}{\Delta\omega_R}(1-i) + \frac{5 \cdot 7}{4}\frac{p_5}{\Delta\omega_R^2}(1+i) \right. \\ &\quad \left. - \frac{5 \cdot 7 \cdot 9}{8}\frac{p_7}{\Delta\omega_R^3}(1-i) - + \cdots\right\}. \end{aligned} \tag{X.25}$$

One recognizes that the first two terms are identical with the first terms in the equations (X.18) and (X.23). Hence, we always obtain the static wing for large $\Delta\omega_R$.

Another important property of $i(\Delta\omega_R)$ is that for small $\Delta\omega_R$ its leading terms in the expansion are

$$i_0(\Delta\omega_R) = \lim_{\Delta\omega_R \to 0} i(\Delta\omega_R) = -\frac{a_1}{\pi}\frac{1}{\Delta\omega_R^2} - i\frac{(a_1 b_1 - a_2)}{\pi \Delta\omega_R} + \cdots. \tag{X.26}$$

In this manner it smoothly goes over to the Lorentz profile of the unmodified impact theory.

Before discussing the numerical results of $i(\Delta\omega_R)$ we first list the constants a_k and b_k for the cases A, B and C as specified at the end of Section IX. a_1 and b_1 are determined from equation (X.8), where p_1 is given by equation (X.5) and p_2 is taken from the large time limit of the computed $\bar{F}(s)$. $p_{2\,\mathrm{comp.}}$ as calculated numerically may differ slightly from p_2 as defined in equation (X.5), if C is not very much smaller than unity because equation (X.5) is only correct for small C. a_2 and b_2 are determined numerically by a least squares fit. The maximum deviations from $\bar{F}(s)$ obtained with $G_1(s)$ alone and with $G_1(s)+G_2(s)$ are listed too. In presenting the numerical results of $i(\Delta\omega_R)$ we concentrate on the real part which turns out to be the most important part. We have chosen two different normalizations. In Figs. 4 and 5, $i(\Delta\omega_R)$ is normalized with respect to the large frequency limit $i_\infty(\Delta\omega_R)$ to show the useful range of the static theory. The short vertical lines mark the position of the Weisskopf frequency

$$\Delta\omega_c = v_{\mathrm{av}}^2 \Big/ \left(\frac{3}{2}(nq_c - n'q_c')\frac{\hbar}{m}\right) = \tilde{\omega}_p/\mathrm{C} \tag{X.27}$$

for a particular component $(nq_c - n'q_c')$ which according to classical arguments determines roughly the range of validity for the static theory (see p. 321 of UNSÖLD, 1955 and paper II). It should be pointed out that $\Delta\omega_c$ is usually defined in terms of an average Stark splitting. In both cases A and C $\Delta\omega_c$ describes the range of the static theory very well. If one allows

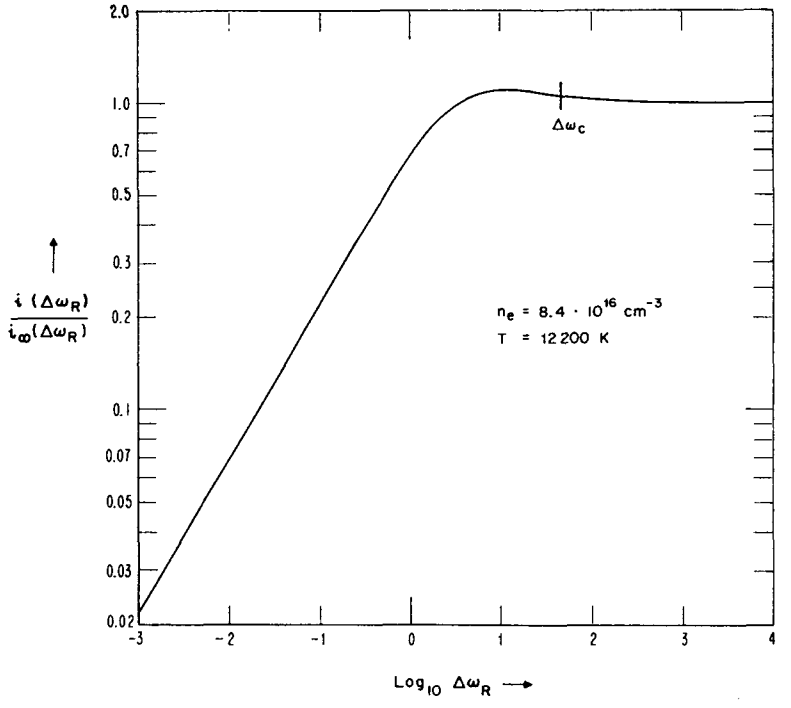

FIG. 4. The Fourier transform of the thermal average i, normalized with respect to the static, large frequency limit i_∞ as a function of the normalized frequency $\Delta\omega_R = (\Delta\omega - \Delta\omega_i \cdot \beta)/\tilde{\omega}_p$. $\Delta\omega_c$ indicates the Weisskopf frequency.

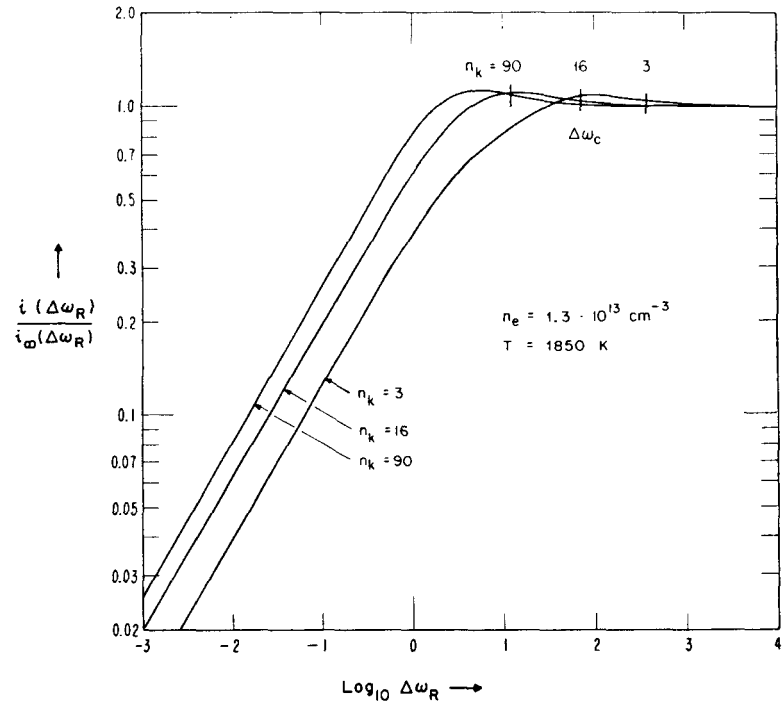

FIG. 5. The Fourier transform of the thermal average i, normalized with respect to the static, large frequency limit i_∞ as a function of the normalized frequency $\Delta\omega_R = (\Delta\omega - \Delta\omega_i \cdot \beta)/\tilde{\omega}_p$. The three different curves correspond to different Stark components characterized by the quantum number $n_k = nq - n'q'$. The short vertical lines give the position of the Weisskopf frequency $\Delta\omega_c$ for every individual component.

for a deviation of about 10 per cent at the most from the static asymptote, $\Delta\omega_c$ may be lowered effectively by more than an order of magnitude. A more detailed discussion is given later with the final line profile calculations.

The other normalization with respect to the small frequency limit $i_0(\Delta\omega_R)$ is shown in Figs. 6 and 7 for cases A and C again. These plots demonstrate the useful range of the unmodified impact theory, which is based on $i_0(\Delta\omega_R)$ and is expected to break down around the plasma frequency, as can be seen in Figs. 6 and 7. In order to extend the range of validity, the modified impact theory makes an impact parameter cutoff at $v/\Delta\omega$ (the Lewis cutoff) whenever this is smaller than the Debye length D; this cutoff accounts for the finite time of interaction to second order. More details are given in the Appendix. The corresponding function $i_{\text{Lewis}}(\Delta\omega_R)$ has been included in Figs. 6 and 7. Since the usual derivation of $i_{\text{Lewis}}(\Delta\omega_R)$ is based on the limit of very small C, one expects the best agreement between the Lewis result and our result, which considers the finite time of interaction to all orders, for the situation with the smallest C. That this is in fact true can be seen from the low density case with $nq_c - n'q'_c = 3$. This component is plotted again in Fig. 8, in order to demonstrate the importance of $G_2(s)$ for those cases where the deviation of $G_1(s)$ from $\bar{F}(s)$ is large (Table 1 gives a maximum deviation of 13 per cent).

Figures 6 and 7 also contain the static limit $i_\infty(\Delta\omega_R)$ (dashed lines) and the Weisskopf frequency $\Delta\omega_c$. It gives an idea how close the Lewis results get to the static limit. One

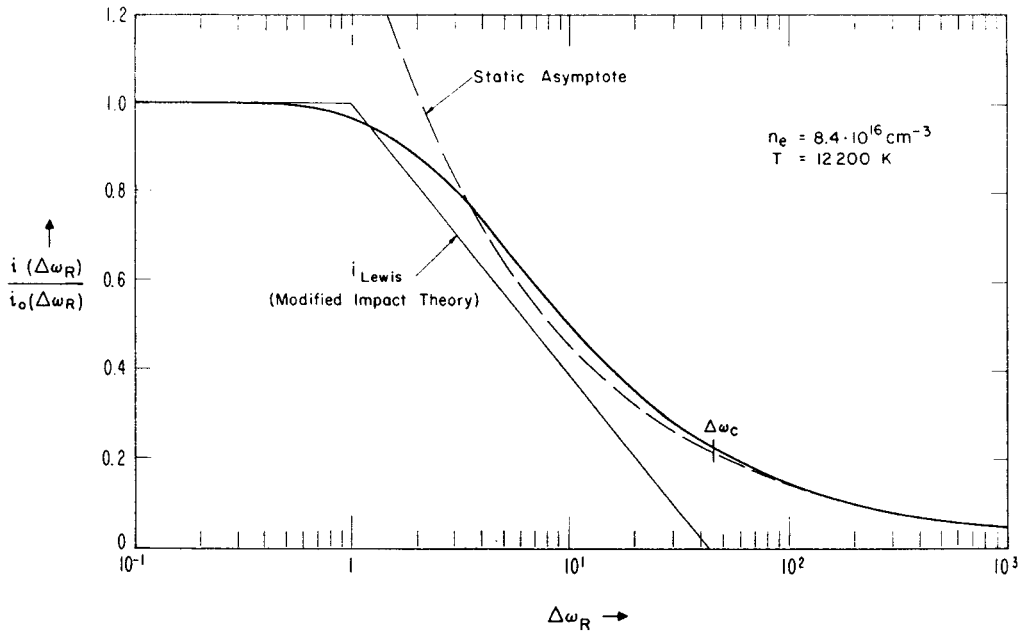

FIG. 6. The Fourier transform of the thermal average i, normalized with respect to the small frequency, impact limit i_0 as a function of the normalized frequency $\Delta\omega_R = (\Delta\omega - \Delta\omega_i\beta)\tilde{\omega}_p$. The static asymptote (dashed line), the Weisskopf frequency $\Delta\omega_c$ and the Fourier transform as used by the modified impact theory are shown.

notices that with increasing values of C the deviation of $i_{\text{Lewis}}(\Delta\omega_R)$ from the static limit becomes larger. In his line wing calculations (GRIEM, 1962, 1967a) GRIEM adjusts his "strong collision term" $E_{\beta\beta'}$ in such a manner that the Lewis result is identical with the static limit at the Weisskopf frequency. In the Figs. 6 and 7 this means that the straight line representing $i_{\text{Lewis}}(\Delta\omega_R)$ is shifted to the right until it cuts $\Delta\omega_c$. We use here $\Delta\omega_c$ as defined in equation (X.27) for every individual component instead of the average value $\Delta\omega_c = kT/(\hbar n^2)$ used by Griem. Since the Lewis line would then lie appreciably above the curve $i(\Delta\omega_R)$ one realizes that this procedure definitely overestimates the electron broadening as already observed experimentally (VIDAL, 1965; see also PFENNIG, TREFFTZ and VIDAL, 1966). A better method would have been to adjust $E_{\beta\beta'}$ such that $i_{\text{Lewis}}(\Delta\omega_R)$ forms a tangent of the static limit. However, it is clear that any adjustment of $E_{\beta\beta'}$ effectively changes the range of the unmodified impact theory and also defeats the purpose of the Lewis cutoff, namely to correct the completed collision assumption to second order.

Finally it ought to be emphasized again that except for the time ordering the Fourier transform of the thermal average $i(\Delta\omega_R)$ as presented here takes into account the *finite* time of interaction to *all* orders. Hence, for small $\Delta\omega_R$ it goes over to the impact theory limit and for large $\Delta\omega_R$ it gives the static limit without requiring a Lewis cutoff.

XI. THE ONE-ELECTRON LIMIT FOR HYDROGEN AND THE ASYMPTOTIC WING EXPANSION

Having obtained the Fourier transform of the thermal average $i(\Delta\omega_R)$ we are now prepared to calculate the actual line intensity by evaluating $I(\omega, \varepsilon_i)$ according to equation

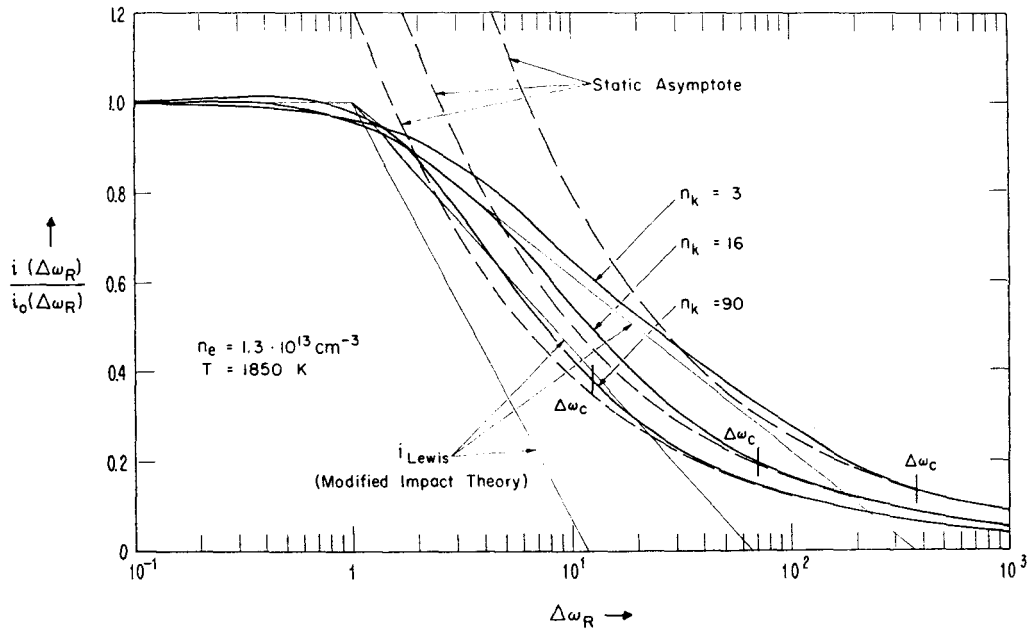

FIG. 7. The Fourier transform of the thermal average i, normalized with respect to the small frequency, impact limit i_0 as a function of the normalized frequency $\Delta\omega_R = (\Delta\omega - \Delta\omega_i\beta)/\tilde{\omega}_p$. The three sets of curves correspond to different Stark components characterized by the quantum number $n_k = nq - n'q'$. The static asymptote (dashed lines), the Weisskopf frequency $\Delta\omega_c$ and the Fourier transform as used by the modified impact theory are shown for every individual component.

(IV.15) and averaging it over all ion fields according to equation (II.1). As explained in Section IV this problem is greatly simplified in the one electron limit where no matrix inversion is required and the intensity $I(\Delta\omega)$ is given by

$$I(\Delta\omega) = I_i(\Delta\omega) + \int_0^\infty P(\beta) I(\Delta\omega, \beta)\, d\beta. \tag{XI.1}$$

TABLE 1. NUMERICAL CONSTANTS FOR THE EXPERIMENTAL CASES, A, B AND C

Case	A	B	C		
	$n_e = 8.4 \cdot 10^{16}\,cm^{-3}$ $T_e = 12\,200K$ $n_k = 2$	$n_e = 3.6 \cdot 10^{17}\,cm^{-3}$ $T_e = 20\,400K$ $n_k = 2$	$n_k = 3$	$n_e = 1.3 \cdot 10^{13}\,cm^{-3}$ $T_e = 1850K$ $n_k = 16$	$n_k = 90$
C	0.02169	0.02685	0.002669	0.01423	0.08006
p_1	−0.05124	−0.07373	−0.01050	−0.1293	−1.725
p_2	−0.03335	−0.04990	$-3.932 \cdot 10^{-3}$	−0.07696	−1.296
$a_1 = p_{2\,comp.}$	−0.03340	−0.05003	$-3.932 \cdot 10^{-3}$	−0.07701	−1.323
b_1	0.2125	0.2303	0.07011	0.1773	0.2941
$\lvert(\bar{F} - G_1)/\bar{F}\rvert$	<0.026	<0.034	<0.13	<0.012	<0.068
a_2	$-3.95 \cdot 10^{-3}$	$-6.57 \cdot 10^{-3}$	$2.38 \cdot 10^{-4}$	$-9.92 \cdot 10^{-3}$	−0.355
b_2	0.539	0.449	0.0664	1.54	0.477
$\lvert(\bar{F} - G_1 - G_2)/\bar{F}\rvert$	<0.004	<0.003	<0.009	<0.013	<0.013

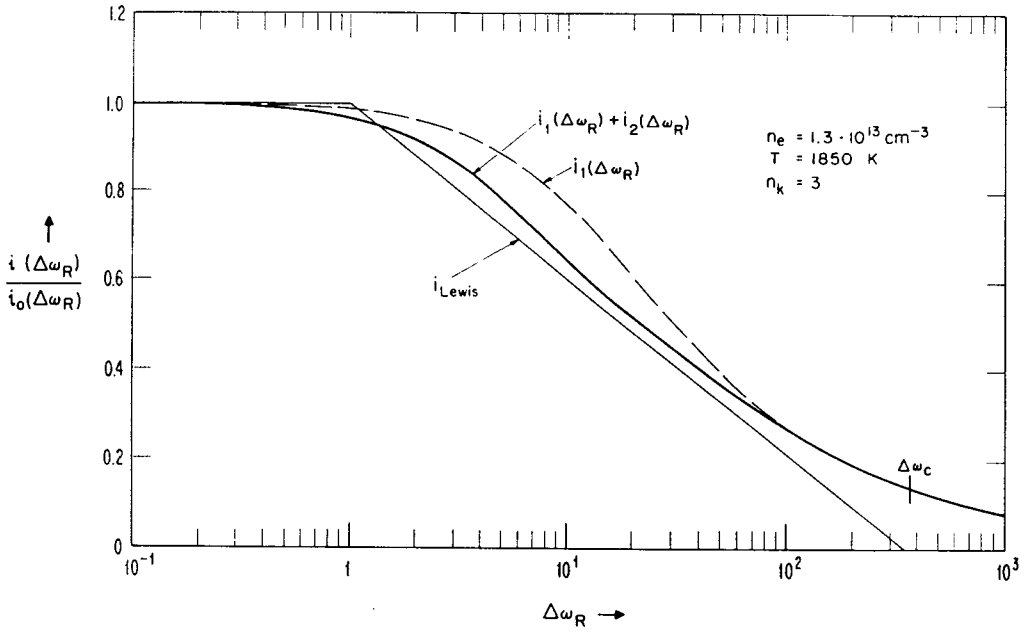

FIG. 8. The Fourier transform of the thermal average i, normalized with respect to the small frequency, impact limit i_0 is shown as a function of the normalized frequency $\Delta\omega_R = (\Delta\omega - \Delta\omega_i\beta)/\bar{\omega}_p$ for a situation where $i_2(\Delta\omega_R)$ (defined in equation (X.22)) represents an important correction. The Fourier transform as used by the modified impact theory is included.

$I_i(\Delta\omega)$ is the static ion contribution originating from the first term, $1/\Delta\omega_{op}$ in equation (IV.21) and $I(\Delta\omega, \beta)$ is given by

$$I(\Delta\omega,\beta) = \frac{\mathrm{Re}}{\pi}\sum \langle nq_am_a|\mathbf{d}|n'q_a'm_a'\rangle\langle n'q_b'm_b'|\mathbf{d}|nq_bm_b\rangle \int \mathrm{d}t\, \exp\{i\Delta\omega_R t\}\langle n'q_b'm_b'; nq_bm_b|\bar{\mathscr{F}}^{(1)}(t)|n'q_a'm_a'; nq_am_a\rangle \qquad \text{(XI.2)}$$

using the definitions of equations (V.14) and (X.2). The density matrix ρ_a is assumed to be constant over the relevant initial states. With equation (IX.1) the last expression can be rewritten as

$$\begin{aligned} I(\Delta\omega,\beta) = \sum & \langle nl_am_a|\mathbf{d}|n'l_a'm_a'\rangle\langle n'q_b'm_b'|n'l_c'm_b'\rangle\langle n'l_c'm_b'|\mathbf{d}|nl_cm_b\rangle\langle nl_cm_b|nq_bm_b\rangle \\ & \times\langle n'l_a'm_c'|n'q_c'm_c'\rangle\langle n'q_c'm_c'|n'l_b'm_c'\rangle\langle n'l_b'm_b'|n'q_b'm_b'\rangle\langle nq_bm_b|nl_bm_b\rangle\langle nl_bm_c|nq_cm_c\rangle \\ & \times\langle nq_cm_c|nl_am_c\rangle(-1)^{-m_a-m_b}(2L+1)\begin{pmatrix} l_a' & l_a & L \\ -m_c' & m_c & M'\end{pmatrix}\begin{pmatrix} l_a' & l_a & L \\ -m_a' & m_a & M\end{pmatrix} \\ & \times\begin{pmatrix} l_b' & l_b & L \\ -m_c' & m_c & M'\end{pmatrix}\begin{pmatrix} l_b' & l_b & L \\ -m_b' & m_b & M\end{pmatrix} i(\Delta\omega_R,\beta,n,n',q_b,q_b',q_c,q_c') \end{aligned} \qquad \text{(XI.3)}$$

where the dipole matrix elements have been transformed from parabolic to spherical states and the summation over intermediate states $|nq_am_a\rangle$ and $|n'q_a'm_a'\rangle$ has been performed. We

next apply the Wigner Eckart theorem (see equation (5.4.1) of EDMONDS, 1960) to the dipole matrix elements and replace the reduced matrix elements by the corresponding radial matrix elements (see BETHE and SALPETER, 1957).

$$\langle nlm|d_\mu|n'l'm'\rangle = (-1)^{-m}\sqrt{[(2l+1)(2l'+1)]}\begin{pmatrix} l & 1 & l' \\ -m & \mu & m' \end{pmatrix}\begin{pmatrix} l & 1 & l' \\ 0 & 0 & 0 \end{pmatrix}\langle nl|r|n'l'\rangle. \qquad \text{(XI.4)}$$

Inserting this relation into equation (XI.3) and using the orthogonality properties of the $3j$-symbols we have

$$\begin{aligned} I(\Delta\omega,\beta) = \sum & \langle n'q_b'm_b'|n'l_c'm_b'\rangle\langle nl_cm_b|nq_bm_b\rangle\langle n'l_a'm_c'|n'q_c'm_c'\rangle\langle n'q_c'm_c'|n'l_b'm_c'\rangle \\ & \times\langle n'l_b'm_b'|n'q_b'm_b'\rangle\langle nq_bm_b|nl_bm_b\rangle\langle nl_bm_c|nq_cm_c\rangle\langle nq_cm_c|nl_am_c\rangle \\ & \times[(2l_a+1)(2l_a'+1)(2l_c+1)(2l_c'+1)]^{1/2}\langle nl_a|r|n'l_a'\rangle\langle n'l_c'|r|nl_c\rangle\begin{pmatrix} l_a' & l_a & 1 \\ 0 & 0 & 0 \end{pmatrix} \\ & \times\begin{pmatrix} l_c' & l_c & 1 \\ 0 & 0 & 0 \end{pmatrix}\begin{pmatrix} l_a' & l_a & 1 \\ -m_c' & m_c & M' \end{pmatrix}\begin{pmatrix} l_b' & l_b & 1 \\ -m_c' & m_c & M' \end{pmatrix}\begin{pmatrix} l_b' & l_b & 1 \\ -m_b' & m_b & M \end{pmatrix} \\ & \times\begin{pmatrix} l_c' & l_c & 1 \\ -m_b' & m_b & M \end{pmatrix} i(\Delta\omega_R,\beta,n,n',q_b,q_b',q_c,q_c'). \end{aligned} \qquad \text{(XI.5)}$$

If we finally replace the unitary transformation by the corresponding $3j$-symbols according to equation (VIII.8) the result is

$$\begin{aligned} I(\Delta\omega,\beta) = \sum & (2l_a+1)(2l_a'+1)(2l_b+1)(2l_b'+1)(2l_c+1)(2l_c'+1)\begin{pmatrix} l_a' & l_a & 1 \\ 0 & 0 & 0 \end{pmatrix}\begin{pmatrix} l_c' & l_c & 1 \\ 0 & 0 & 0 \end{pmatrix} \\ & \times\begin{pmatrix} l_a' & l_a & 1 \\ -m_c' & m_c & M' \end{pmatrix}\begin{pmatrix} l_b' & l_b & 1 \\ -m_c' & m_c & M' \end{pmatrix}\begin{pmatrix} l_b' & l_b & 1 \\ -m_b' & m_b & M \end{pmatrix}\begin{pmatrix} l_c' & l_c & 1 \\ -m_b' & m_b & M \end{pmatrix} \\ & \times\begin{pmatrix} \frac{n-1}{2} & \frac{n-1}{2} & l_b \\ \frac{m_b-q_b}{2} & \frac{m_b+q_b}{2} & -m_b \end{pmatrix}\begin{pmatrix} \frac{n-1}{2} & \frac{n-1}{2} & l_c \\ \frac{m_b-q_b}{2} & \frac{m_b+q_b}{2} & -m_b \end{pmatrix}\begin{pmatrix} \frac{n-1}{2} & \frac{n-1}{2} & l_a \\ \frac{m_c-q_c}{2} & \frac{m_c+q_c}{2} & -m_c \end{pmatrix} \\ & \times\begin{pmatrix} \frac{n-1}{2} & \frac{n-1}{2} & l_b \\ \frac{m_c-q_c}{2} & \frac{m_c+q_c}{2} & -m_c \end{pmatrix}\begin{pmatrix} \frac{n'-1}{2} & \frac{n'-1}{2} & l_b' \\ \frac{m_b'-q_b'}{2} & \frac{m_b'+q_b'}{2} & -m_b' \end{pmatrix}\begin{pmatrix} \frac{n'-1}{2} & \frac{n'-1}{2} & l_c' \\ \frac{m_b'-q_b'}{2} & \frac{m_b'+q_b'}{2} & -m_b' \end{pmatrix} \\ & \times\begin{pmatrix} \frac{n'-1}{2} & \frac{n'-1}{2} & l_a' \\ \frac{m_c'-q_c'}{2} & \frac{m_c'+q_c'}{2} & -m_c' \end{pmatrix}\begin{pmatrix} \frac{n'-1}{2} & \frac{n'-1}{2} & l_b' \\ \frac{m_c'-q_c'}{2} & \frac{m_c'+q_c'}{2} & -m_c' \end{pmatrix}\langle nl_a|r|n'l_a'\rangle\langle n'l_c'|r|nl_c\rangle \\ & \times i(\Delta\omega_R,\beta,n,n',q_b,q_b',q_c,q_c'). \end{aligned} \qquad \text{(XI.6)}$$

The preceding relations hold for the general case of upper and lower state interactions. They simplify considerably if there is no lower state interaction (e.g. Lyman lines). Then one obtains

$$I_u(\Delta\omega,\beta) = |\langle n1|r|10\rangle|^2 \sum_{\substack{m_b,m_c\\ q_b,q_c}} \begin{pmatrix} \frac{n-1}{2} & \frac{n-1}{2} & 1 \\ \frac{m_b-q_b}{2} & \frac{m_b+q_b}{2} & -m_b \end{pmatrix}^2 \begin{pmatrix} \frac{n-1}{2} & \frac{n-1}{2} & 1 \\ \frac{m_c-q_c}{2} & \frac{m_c+q_c}{2} & -m_c \end{pmatrix}^2$$

$$\times\, i_u(\Delta\omega_R,\beta,n,q_b,q_c) \tag{XI.7}$$

with

$$i_u(\Delta\omega_R,\beta,n,q_b,q_c) = i(\Delta\omega_R,\beta,n,n'=1,q_b,q_b'=0,q_c,q_c'=0). \tag{XI.8}$$

Equation (XI.7) may be further simplified by evaluating the 3j-symbols and summing over m_b and m_c with the result.

$$I_u(\Delta\omega,\beta) = \frac{|\langle n1|r|10\rangle|^2}{4(n^2-1)^2n^2} \sum_{q_b=-(n-1)}^{n-1} [n^2+(-1)^{q_b+n}(n^2-2q_b^2)]$$

$$\times \sum_{q_c=-(n-1)}^{n-1} [n^2+(-1)^{q_c+n}(n^2-2q_c^2)]\, i_u(\Delta\omega_R,\beta,n,q_b,q_c). \tag{XI.9}$$

These simplified relations may also be used for the higher series members of the other series, whose transitions do not end on the ground state if lower state interactions contribute only a negligible amount of broadening to the final line profile.

The foregoing relations for the one electron limit essentially represent the asymptotic expression for the intensity in the line wings. If one is interested in frequency perturbations $\Delta\omega$ which are significantly larger than the average ion field splitting equation (XI.1) can be simplified by replacing the ion field average of the electron contribution by the electron contribution for the average ion field β_{av}

$$I(\Delta\omega) = I_i(\Delta\omega) + I(\Delta\omega,\beta_{av}) \tag{XI.10}$$

with

$$\beta_{av} = \int_0^\infty \beta W(\beta)\,\mathrm{d}\beta. \tag{XI.11}$$

If $\Delta\omega$ is very much larger than the average ion field splitting, then according to equation (X.2) $\Delta\omega_R \simeq \Delta\omega/\tilde{\omega}_p$ and $I(\Delta\omega,\beta_{av})$ may be replaced by $I(\Delta\omega,\beta=0)$.

$$I(\Delta\omega) = I_i(\Delta\omega) + I(\Delta\omega,\beta=0). \tag{XI.12}$$

In the limit $\beta \to 0$ the equations (XI.5) to (XI.9) simplify drastically because $i(\Delta\omega_R)$ depends no longer on the quantum numbers q_b and q_b' which specify the Stark components shifted by the quasistatic ion fields. This allows us to sum in equation (XI.7) over q_b and m_b which

gives us for the case of no lower state interaction

$$I_u(\Delta\omega, \beta = 0) = |\langle n1|r|10\rangle|^2 \sum_{qm} \begin{pmatrix} \frac{n-1}{2} & \frac{n-1}{2} & 1 \\ \frac{m-q}{2} & \frac{m+q}{2} & m \end{pmatrix} i_u(\Delta\omega, \beta = 0, n, q)$$

$$= \frac{|\langle n1|r|10\rangle|^2}{2(n^2-1)n} \sum_{q=-(n-1)}^{(n-1)} (n^2 + (-1)^{q+n}(n^2 - 2q^2)) i_u(\Delta\omega, \beta = 0, n, q). \qquad \text{(XI.13)}$$

For the general case of upper and lower state interaction we can sum in equation (XI.6) over q_b, q_b', m_b, m_b' and M and after applying equation (XI.4) we finally sum over the intermediate spherical states to obtain

$$I(\Delta\omega, \beta = 0) = \sum_{\substack{q,q' \\ m,m'}} |\langle nqm|\mathbf{d}|n'q'm'\rangle|^2 i(\Delta\omega, \beta = 0, n, n', q, q'). \qquad \text{(XI.14)}$$

How far into the line center the simplified relations (XI.10) and (XI.12) may be used, depends on the required accuracy. Numerical results, which compare the asymptotic wing expansions with the more rigorous unified theory calculations describing the entire line profile, are given at the end of the next section.

XII. THE UNIFIED THEORY FOR HYDROGEN

In those cases, where the entire line profile including the line center is required, the line intensities have to be calculated on the basis of the unified theory. It has to be pointed out that in principal even in calculating the distant line wings the unified theory has to be used whenever $\Delta\omega_R$ in equations (X.1) or (V.17) is no longer large compared to unity. This will happen in the final integration over ion fields whenever β is close to

$$\beta_c = \Delta\omega/\Delta\omega_i(n, q_b, n', q_b'). \qquad \text{(XII.1)}$$

However, it was shown in the last section, that for large $\Delta\omega$ one may use one of the asymptotic expansions in equations (XI.10) and (XI.12).

In the unified theory we have to evaluate the following expression

$$I(\Delta\omega, \beta) = \frac{Im}{\pi} \sum \langle nq_a m_a|\mathbf{d}|n'q_a'm_a'\rangle \langle n'q_b'm_b'|\mathbf{d}|nq_b m_b\rangle$$
$$\times \langle n'q_b'm_b'; nq_b m_b|[\Delta\omega_{op} - \mathscr{L}(\Delta\omega_{op})]^{-1}|n'q_a'm_a'; nq_a m_a\rangle. \qquad \text{(XII.2)}$$

The matrix elements of $\Delta\omega_{op}$ as defined in equation (IV.14) are diagonal in parabolic states and are given by

$$\langle n'q_a'm_a'; nq_a m_a|\Delta\omega_{op}|n'q_a'm_a'; nq_a m_a\rangle = \Delta\omega - \Delta\omega_i(n, q_a, n', q_a')\beta \qquad \text{(XII.3)}$$

where $\Delta\omega_i$ is defined in equation (V.14). The matrix elements of $\mathscr{L}(\Delta\omega_{op})$ are given by

$$\begin{aligned}\langle n'q_b'm_b'; nq_bm_b|\mathscr{L}(\Delta\omega_{op})|nq_a'm_a'; nq_am_a\rangle &= -i\pi\cdot(-1)^{-m_a-m_b}[\Delta\omega-\Delta\omega_i(n,q_b,n',q_b')\beta]^2\\ &\times\sum(2L+1)\langle n'q_a'm_a'|n'l_a'm_a'\rangle\langle n'l_a'm_c'|n'q_c'm_c'\rangle\langle n'q_c'm_c'|n'l_b'm_c'\rangle\langle n'l_b'm_b'|n'q_b'm_b'\rangle\\ &\times\langle nq_am_a|nl_am_a\rangle\langle nl_am_c|nq_cm_c\rangle\langle nq_cm_c|nl_bm_c\rangle\langle nl_bm_b|nq_bm_b\rangle\begin{pmatrix} l_a' & l_a & L\\ -m_c' & m_c & M'\end{pmatrix}\\ &\times\begin{pmatrix} l_a' & l_a & L\\ -m_a' & m_a & M\end{pmatrix}\begin{pmatrix} l_b' & l_b & L\\ -m_c' & m_c & M'\end{pmatrix}\begin{pmatrix} l_b' & l_b & L\\ -m_b' & m_b & M\end{pmatrix}i(\Delta\omega_R,\beta,n,n',q_b,q_b',q_c,q_c')\end{aligned}\tag{XII.4}$$

using equations (IV.16), (IX.1) and (X.1). This relation simplifies significantly in case of no lower state interaction in which case we need the matrix elements

$$\begin{aligned}\langle nq_bm_b|\mathscr{L}(\Delta\omega_{op})|nq_am_a\rangle &= -i\pi[\Delta\omega-\Delta\omega_i(n,q_b)\beta]^2\sum_{l_a,q_c,m_c}\frac{\delta_{m_am_b}}{2l_a+1}\langle nq_bm_b|nl_am_a\rangle\\ &\times\langle nl_am_a|nq_am_a\rangle[\langle nl_am_c|nq_cm_c\rangle]^2 i_u(\Delta\omega_R,\beta,n,q_b,q_c).\end{aligned}\tag{XII.5}$$

Due to the delta function the matrix of the operator $\mathscr{L}$ is then block diagonal in m, which reduces the size of the matrices to be inverted to $n\times n$ or $(n-1)\times(n-1)$ depending on the quantum numbers n and m. Furthermore, equation (XII.2) simplifies in case of no lower state interaction. After transforming the dipole matrix elements from parabolic to spherical states, applying the Wigner–Eckart theorem (see equation (XI.4)) and using equation (VIII.8) one obtains

$$\begin{aligned}I(\Delta\omega,\beta) = |\langle n1|r|10\rangle|^2\sum_{q_a,q_b,m}(-1)^{n+m-1-(q_a+q_b)/2}&\begin{pmatrix}\frac{n-1}{2} & \frac{n-1}{2} & 1\\ \frac{m-q_a}{2} & \frac{m+q_a}{2} & -m\end{pmatrix}\\ \times\begin{pmatrix}\frac{n-1}{2} & \frac{n-1}{2} & 1\\ \frac{m-q_b}{2} & \frac{m+q_b}{2} & -m\end{pmatrix}&\frac{Im}{\pi}\langle nq_bm|[\Delta\omega_{op}-\mathscr{L}(\Delta\omega_{op})]^{-1}|nq_am\rangle.\end{aligned}\tag{XII.6}$$

In order to keep the mathematics simpler we concentrate in the following on the case of no lower state interaction, because it covers the experimental situations of case A and B and is also a good approximation to the higher Balmer lines of case C (see the list of references at the end of Section IX). Including lower state interactions means at this stage only a more extensive summation over $3j$-symbols because the crucial function $i(\Delta\omega_R,\beta)$, the Fourier transform of the thermal average, has already been evaluated for the general case of upper and lower state interactions.

Using the unitary transformation of equation (VIII.8), equation (XII.5) may be rewritten as

$$\langle nq_b m|\mathscr{L}(\Delta\omega_{\rm op})|nq_a m\rangle = -i\pi(-1)^{n+m-1-(q_a+q_b)/2}[\Delta\omega-\Delta\omega_i(n,q_b)\beta]^2\sum_{l_a}(2l_a+1)$$
$$\times\begin{pmatrix}\frac{n-1}{2} & \frac{n-1}{2} & l_a\\ \frac{m-q_a}{2} & \frac{m+q_a}{2} & -m\end{pmatrix}\begin{pmatrix}\frac{n-1}{2} & \frac{n-1}{2} & l_a\\ \frac{m-q_b}{2} & \frac{m+q_b}{2} & -m\end{pmatrix}2\sum_{q_c>0} i_u(\Delta\omega_R,\beta,n,q_b,q_c)$$
$$\times\sum_{m_c}\begin{pmatrix}\frac{n-1}{2} & \frac{n-1}{2} & l_a\\ \frac{m_c-q_c}{2} & \frac{m_c+q_c}{2} & -m_c\end{pmatrix}^2 \qquad \text{(XII.7)}$$

where we have used the fact that $i_u(\Delta\omega_R,\beta,n,q_b,q_c) = i_u(\Delta\omega_R,\beta,n,q_b,-q_c)$ and that $i_u(\Delta\omega_R,\beta,n,q_b,q_c=0)=0$. We also realize that

$$\langle nq_b-m|\mathscr{L}(\Delta\omega_{\rm op})|nq_a-m\rangle = \langle nq_b m|\mathscr{L}(\Delta\omega_{\rm op})|nq_a m\rangle. \qquad \text{(XII.8)}$$

$I(\Delta\omega,\beta)$ as defined by equations (XII.6) and (XII.7) has been evaluated numerically and the computer program, which also performs the final ion field average, is presented in the report of VIDAL, 1970. The ion microfield distribution function employed is the one given by HOOPER, 1968a, 1968b, which differs less than about 1 per cent from the values determined independently by PFENNIG and TREFFTZ, 1966.

For the experimental parameters of case C, Figs. 9 and 10 show numerical results of $I(\Delta\omega,\beta=10)$ for $n=6$ and $n=10$. The fat vertical lines indicate the relative intensities and the positions of the Stark components for the static field (ion field) $\beta=10$ and it demonstrates the electron broadening.

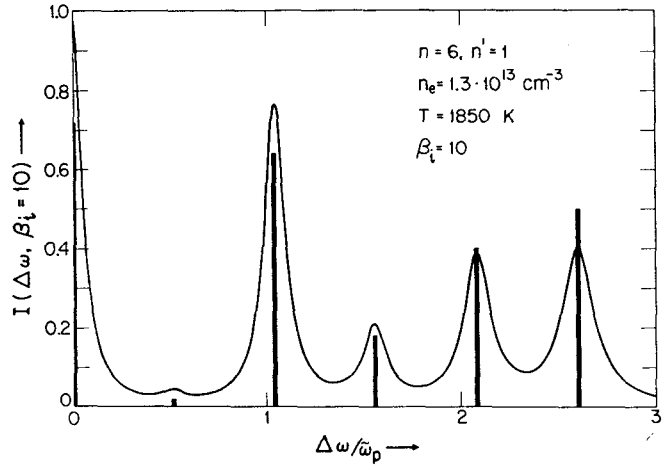

FIG. 9. The intensity profile of the Ly_6-line is shown before the final ion field average for a normalized ion field $\beta_i = 10$ demonstrating the electron broadening.

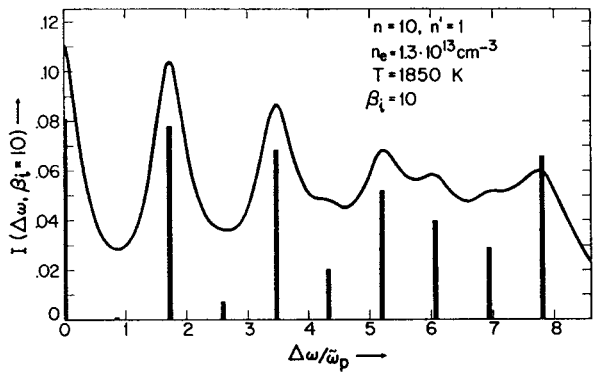

FIG. 10. The intensity profile of the Ly_{10}-line is shown before the final ion field average for a normalized ion field $\beta_i = 10$ demonstrating the electron broadening.

Figures 11–13 show the final line profiles $I(\Delta\omega)$ after performing the ion field average for the experimental cases A, B and C (see end of Section IX). As a first result it turns out that for numerical accuracies of about 2 per cent it is in all 3 cases sufficient to consider only $G_1(t)$ meaning that $i(\Delta\omega_R, \beta, n, q_b, q_c)$ may be replaced by $i_1(\Delta\omega_R, \beta, n, q_b, q_c)$ as given in equation (X.17). Although according to Table 1, $G_1(t)$ may differ from $\bar{F}(t)$ for some components of case C by up to 13 per cent, it turns out that after summing over all Stark components and averaging over ion fields this difference $\bar{F}(t) - G_1(t)$ is apparently smeared out over the entire line profile and affects the final line profile by not more than about 2 per cent. This is very convenient for practical calculations, because it no longer requires an extensive evaluation of the thermal average anymore, but for most practical situations it is sufficient to calculate the line intensities directly on the basis of $G_1(t)$ whose specifying constants a_1 and b_1 are given immediately by the equations (X.8) and (X.5).

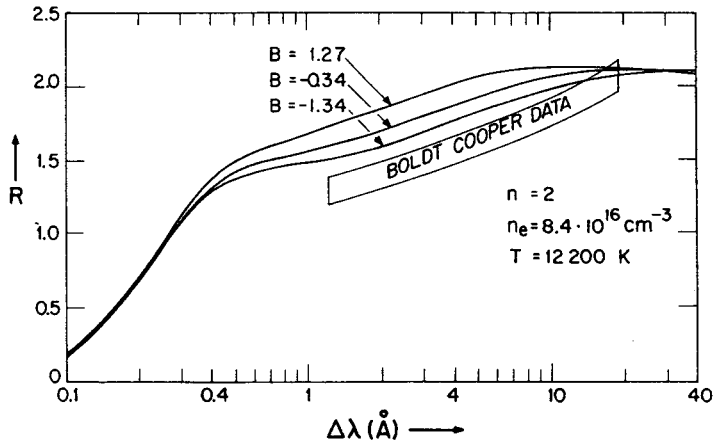

FIG. 11. The final Lyman-α profile normalized with respect to the asymptotic Holtsmark $\Delta\lambda^{-5/2}$-wing (ions only) for three different values of the constant B: 1.27 (KEPPLE and GRIEM, 1968), -0.34 (as derived in this paper for $\rho_{min} = \lambda + \frac{3}{2}n^2a_0$ and $\rho_{max} = D$) and -1.34 (for $\rho_{min} = \lambda + \frac{3}{2}n^2a_0$ and $\rho_{max} = 0.6D$ as proposed by CHAPPELL, COOPER and SMITH, 1969). The data are from the experiment of BOLDT and COOPER, 1964.

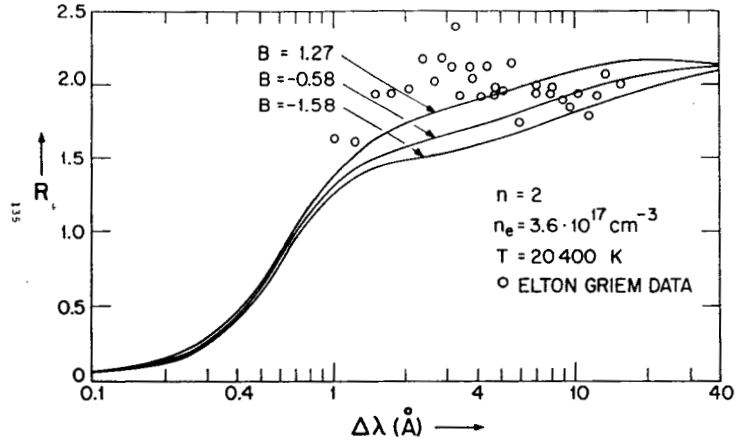

FIG. 12. The final Lyman-α profile normalized with respect to the asymptotic Holtsmark $\Delta\lambda^{-5/2}$-wing (ions only) for three different values of the constant B as explained in the caption of Fig. 11. The data points of ELTON and GRIEM, 1964, are given.

This is even more true in view of the fact that the final line profile is partially affected by an uncertainty in the constant B as defined in equation (IX.31). As summarized in Table 2 of the Appendix its actual value depends on the cutoff procedure applied, a problem which has not yet been solved satisfactorily. The upper cutoff parameter $a = \rho_{max}/D$ (see the

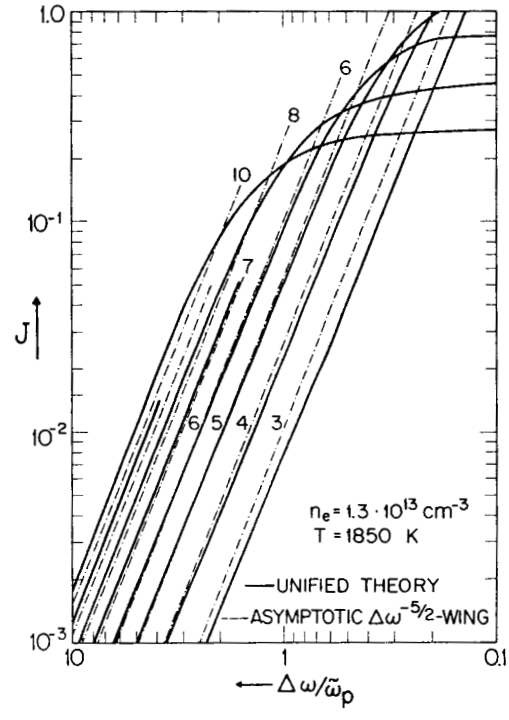

FIG. 13. The final line profiles for the density and temperature parameters of VIDAL, 1965. The asymptotic Holtsmark $\Delta\lambda^{-5/2}$-wings for electrons and ions (dashed lines) are included.

Appendix) and therefore also the limits on the integral $\int PV_c(t')\,dt'$ can in principal be decided within the frame work of the classical path theory (see also CHAPPELL, COOPER and SMITH, 1969). The lower cutoff parameter, however, which essentially replaces the dynamic strong collisions not amenable in a classical path theory, can only be determined conclusively from a quantum mechanical theory which is also able to handle strong collisions and which does not yet exist. The constant B adopted here is based on a lower cutoff parameter $\rho_{min} = \lambda\!\!\!^{-} + \frac{3}{2}n^2a_0$, which specifies approximately the region of validity for the classical path theories (see paper I). This is also the constant used in the Lyman-α calculations of paper III. Numerical results based on other values for the constant B as used in the literature (see summary of the Appendix) are also included in Figs. 11 and 12 for the cases A and B. The largest value $B = 1.27$ is the one adopted in the recent calculations of KEPPLE and GRIEM, 1968, while the smallest value of B is obtained for $\rho_{min} = \lambda\!\!\!^{-} + \frac{3}{2}n^2a_0$ and choosing an upper cutoff of $\rho_{max} = 0.606D$ as proposed by CHAPPELL, COOPER and SMITH, 1969. For case C this variation of the constant B does not show up in Fig. 13 and amounts to an intensity change of at the most about 4 per cent. These variations indicate the reliability of the classical path theories and demonstrate that for some cases the error estimates given in the literature are too optimistic. The effect on the final line profile due to the uncertainty of the constant B will be small if either according to equation (IX.31)

$$-2\ln(2C) \gg 1 \tag{XII.9}$$

or if (like for the higher series members) the number of Stark components is large which tends to smear out the influence of the constant B. It should be pointed out again that the unified theory is intrinsicly normalized independent of the value of the specifying constants of a particular line. Hence, any variation of the constant B does not affect the normalization of the line profile.

In his unified approach to Stark broadening VOSLAMBER also presents calculations for the case A, which show better agreement with the experiment than the calculations presented in Fig. 11. We have unsuccessfully tried to reproduce his calculations making the same set of approximations which essentially amounts to calculating the line intensity on the basis of equation (XI.12) where the total intensity is given as a sum of the static ion part $I_i(\Delta\omega)$ and the electron contribution $I(\Delta\omega, \beta = 0)$ neglecting the ion field splitting (see the dashed curve for $\beta = 0$ in Fig. 17). While the calculations of the thermal average presented here have been obtained by straightforward integration of equation (IX.2), his calculations are based on the Monte Carlo method. Numerical round off errors, which can easily be overlooked, have been avoided in the calculations presented here by the use of seven different expansions for the various limits of the function Φ in equation (IX.3) (see Appendix A of the NBS Monograph, VIDAL, COOPER and SMITH, 1970).

In comparing the numerical results for case C, with the experiment it has to be kept in mind that we are comparing the higher Balmer lines with calculations for the higher Lyman lines, because our final line profile calculations have not yet taken into account lower state interactions. This means that in a plot of the intensity versus the wavenumbers $\Delta\bar{\nu}$, which is essentially an energy scale, the line profiles cannot be expected to coincide because of the difference in the Stark effect. This gives rise to different static wings as explained in detail by VIDAL, 1965. Hence, we have to rescale the Lyman profiles preserving normalization in order to be able to compare the measured profiles of the Balmer lines with the calculated profiles of the Lyman lines. This means that in a plot of $\log I$ versus $\log \Delta\bar{\nu}$ we can compare

the line shape of the corresponding lines directly. The agreement is remarkable. For the higher lines, $n \geq 8$, where Doppler broadening was shown to be negligible and where lower state interactions no longer affect the line shape noticeably, the agreement is better than 2 per cent over the entire measured line profile, which for $n = 8$ extends over 3 orders of magnitude in intensity. In particular, the calculations show also the surprisingly large range of the $\Delta\omega^{-5/2}$-wing, which extends to 1/10 of the maximum intensity. This fact is not explainable by a purely static theory considering also shielding effects. (See PFENNIG, 1966.) For the lower lines the calculated profiles have to be folded into a Doppler profile in order to achieve similarly good agreement. For the lower line we also expect in the line center some influence due to lower state interactions on the line shape which is partially removed again by Doppler broadening.

A more detailed study of the $\Delta\omega^{-5/2}$-wings reveals some other interesting facts. In Fig. 13, the dashed lines indicate the asymptotic $\Delta\omega^{-5/2}$-wings; except for $n = 5$ and $n = 6$, what appears to be a $\Delta\omega^{-5/2}$-wing in the measurements and calculations is not the asymptotic Holtsmark $\Delta\omega^{-5/2}$-wing in the region of interest. If one extends the calculations to even larger frequencies $\Delta\omega$, all the wings will eventually coincide with their asymptotic limit. In the paper of VIDAL, 1965, Table II gives a list of the electron densities, which were evaluated under the erroneous assumption that the measured $\Delta\omega^{-5/2}$-wing was the asymptotic Holtsmark wing; it was stated that for H_4 to H_{14} the electron densities coincide with ± 4 per cent. A more careful analysis of the values, which have been plotted again in Fig. 14, reveals

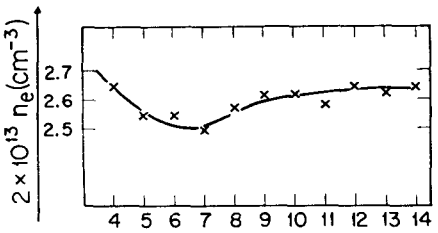

FIG. 14. Plot of the electron density values as a function of the principal quantum number n, which have been evaluated by VIDAL, 1965, under the assumption that the $\Delta\lambda^{-5/2}$-wing revealed by the experiment is identical with the asymptotic Holtsmark $\Delta\lambda^{-5/2}$-wing for electrons and ions.

a systematic trend. For large and very small principal quantum numbers the electron density values rise above the average value, while the minimum value was obtained for $n = 7$. From Fig. 13, it now becomes apparent that the electron densities based on the asymptotic Holtsmark wing will go up for increasing n. For smaller n the quantum number dependence of the electron density is masked by Doppler broadening which raises the wings again and explains the increasing values of electron density for small n. Another important result can be seen from Fig. 13. For small principal quantum numbers the line intensities are much smaller than predicted by a quasistatic theory. This was observed first by SCHLÜTER and AVILA, 1966 and the effective electron densities for a quasistatic theory as a function of $\Delta\lambda$ show the qualitative behavior measured by them after unfolding the Doppler broadening. This observation together with the measurements of BOLDT and COOPER, 1964, suggested the semiempirical procedure proposed by EDMONDS, SCHLÜTER and WELLS,

1967. A detailed quantitative comparison requires for the first series members a consideration of lower state interactions, which is in process.

For the parameters of case C, KEPPLE and GRIEM, 1968, have already calculated the lines H_6 and H_7. These calculations have been extended to H_{12} by BENGTSON, KEPPLE and TANNICH, 1969, using identically the same computer program. The results are plotted in Fig. 15 and comparing the line shape for the higher series members, for which lower state interaction becomes negligible, with our results in Fig. 13 one realizes a significant difference. In particular, their calculations do not reveal the $\Delta\lambda^{-5/2}$ decay in the near line wing for intensities smaller than about $\frac{1}{10}$ of the maximum intensity at $\Delta\omega = 0$ which is discussed above. It should be pointed out that the ion field dependent cutoff, which has been introduced by KEPPLE and GRIEM, 1968, to account for the usually neglected exponential in equation (VI.4) cannot be responsible for it. This has been tested in our calculations. One can understand this by realizing that for the higher series members the effect of dynamic broadening due to the electrons as described roughly by the constants p_2 in equation (X.5) turns out to be much smaller than the halfwidth of the total line, which is essentially determined by quasistatic broadening.

As another interesting result, Fig. 16 shows a plot of a calculated Lyman-β profile for two different values of the constant $B(B = 1.27$ and B for $\rho_{\min} = \hat{\lambda} + \frac{3}{2}n^2 a_0)$, which allows also some qualitative statements concerning H_β. We realize that changing B affects the very line center, where the profile shows the two humps and the near line wing, but it does not change the intensity around the halfwidth significantly, which may be understood

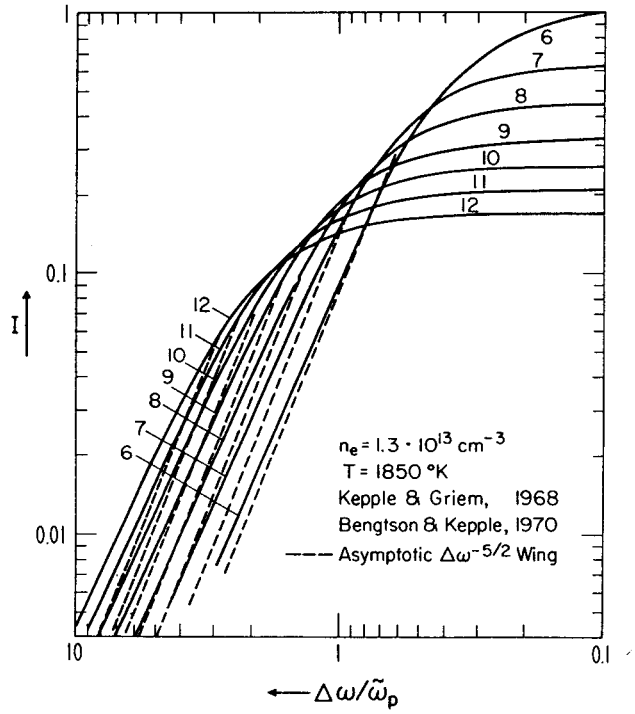

FIG. 15. The Balmer line profiles for the density and temperature parameters of VIDAL, 1965, as calculated by KEPPLE and GRIEM, 1968, and by BENGTSON, KEPPLE and TANNICH, 1969.

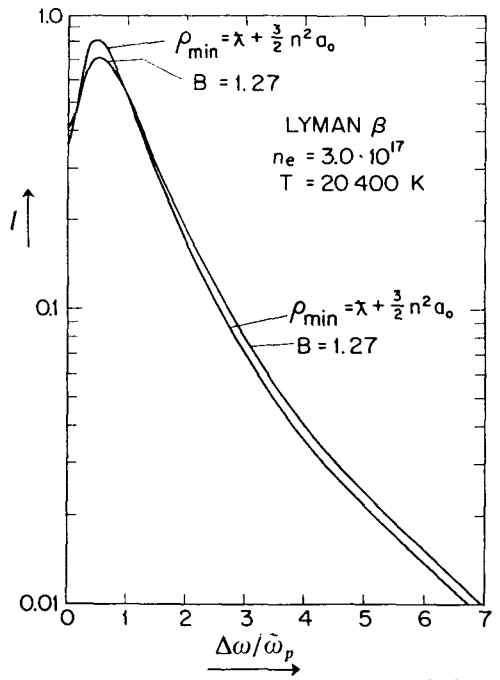

FIG. 16. The Lyman-β profile for two different strong collision cutoffs ρ_{min}.

as an effect of the normalization. This is in agreement with experimental observations of WENDE, 1967, which show that the calculations of GRIEM, KOLB and SHEN, 1962, overestimate the near line wing. It also explains the good agreement of experimental and theoretical halfwidths in high density plasmas (see GERARDO and HILL, 1966) because the line intensity around the halfwidth is rather insensitive to the exact value of B.

Finally, in Figs. 17–19, we compare the unified theory calculations (solid curves) with calculations based on the one-electron theory in order to see how far into the line center

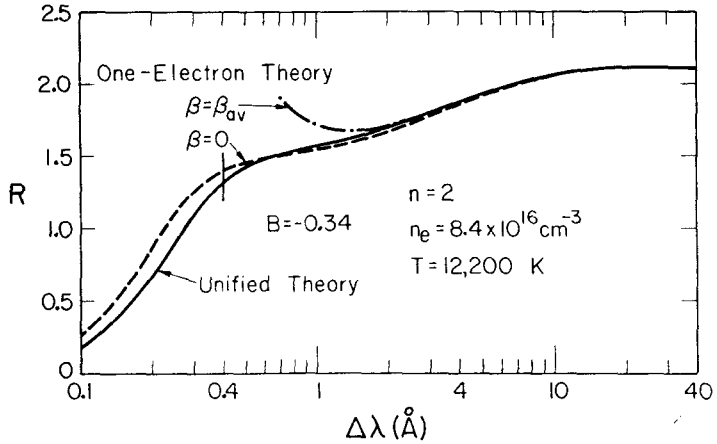

FIG. 17. Comparison of the unified theory calculations with the one-electron theory calculations for Lyman-α. The vertical line marks the position of the shifted Stark component for an ion field $\beta = \beta_{av}$.

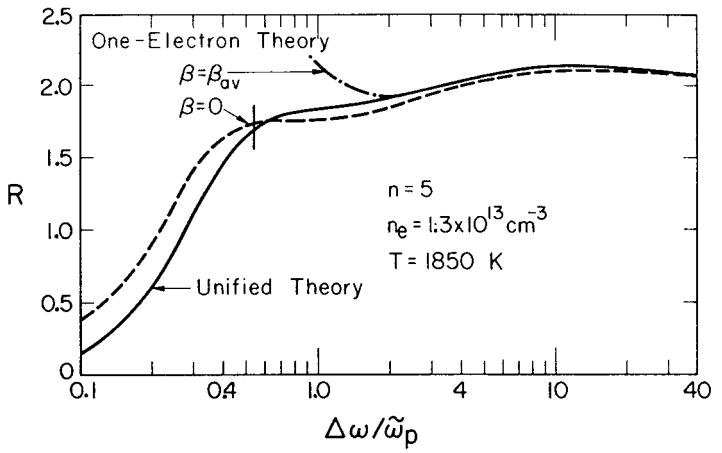

FIG. 18. Comparison of the unified theory calculations with the one-electron theory calculations for $n = 5$. The vertical line marks the position of the outermost, shifted Stark component for an ion field $\beta = \beta_{av}$.

the asymptotic wing expansions as given in equation (XI.10) or (XI.12) may be used. In all Figures the short vertical line indicates the position of the outermost, unperturbed Stark component for an average ion field β_{av}, which is given by $\Delta\omega = \beta_{av}\Delta\omega_i\,(n, q = n-1)$ where $\Delta\omega_i$ is defined in equation (V.14). The dashed lines correspond to the one-electron theory calculations for $\beta = 0$ according to equation (XI.12), while the dash-dotted lines give the results for $\beta = \beta_{av}$ according to equation (XI.10). First of all we realize that, as expected, the one-electron result for $\beta = \beta_{av}$ diverges when $\Delta\omega$ approaches $\beta_{av}\Delta\omega_i(n, q = n-1)$. However, in all three cases we see that for frequencies

$$\Delta\omega \gtrsim 5\beta_{av}\Delta\omega_i\,(n, q = n-1) \tag{XII.10}$$

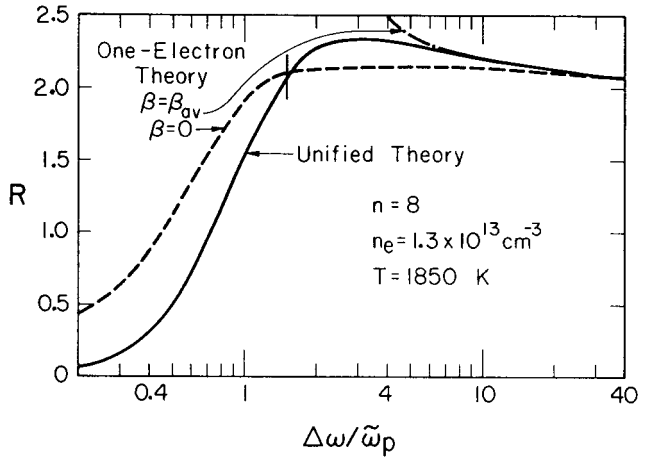

FIG. 19. Comparison of the unified theory calculations with the one-electron theory calculations for $n = 8$. The vertical line marks the position of the outermost, shifted Stark component for an ion field $\beta = \beta_{av}$.

the one-electron theory calculations according to equation (XI.10) coincide with the unified theory calculations to within 1 per cent and better. For slightly released accuracy requirements one may also apply the simpler one-electron theory calculations based on equation (XI.12) with $\beta = 0$. In particular we see that for small principal quantum numbers the useful range is very much larger than for the one-electron theory calculations with $\beta = \beta_{av}$ because, for $\beta = 0$, the one-electron theory diverges only at $\Delta\omega = 0$. We also realize that for the line intensity range of practical interest both asymptotic wing expressions with $\beta = 0$ and $\beta = \beta_{av}$ become less useful with increasing principal quantum number.

REFERENCES

F. ABRAMOWITZ and I. A. STEGUN, *Handbook of Mathematical Functions*, Eds. M. ABRAMOWITZ and I. A. STEGUN (*NBS Appl. Math. Ser.* **55,** 1969).
P. W. ANDERSON and J. D. TALMAN, *Proceedings of the Conference on the Broadening of Spectral Lines*, p. 29, Pittsburgh (1955); also Bell Telephone System Monograph 3117.
M. E. BACON and D. F. EDWARDS, *Phys. Rev.* **170,** 125 (1968).
M. BACON, K. Y. SHEN and J. COOPER, *Phys. Rev.* **188,** 50 (1969).
M. BARANGER, *Phys. Rev.* **111,** 494 (1958); **112,** 855 (1958).
M. BARANGER and B. MOZER, *Phys. Rev.* **115,** 521 (1959); **118,** 626 (1960).
M. BARANGER, *Atomic and Molecular Processes*, p. 493, Ed. D. R. BATES, Academic Press, New York (1962).
H. BATEMAN, *Higher Transcendental Functions*, Vol. II, McGraw-Hill, New York (1953).
R. D. BENGTSON, P. KEPPLE and J. D. TANNICH, *Phys. Rev.* **A1,** 532 (1970).
A. BETHE and E. SALPETER, *Quantum Mechanics of One- and Two-Electron Atoms*, Springer, Berlin (1957).
J. W. BIRKELAND, J. P. OSS and W. G. BRAUN, *Phys. Rev.* **178,** 368 (1969).
G. BOLDT and W. S. COOPER, *Z. Naturforsch.* **19a,** 968 (1964).
W. R. CHAPPELL, J. COOPER and E. W. SMITH, *JQSRT* **9,** 149 (1969).
J. COOPER, *Phys. Rev. Letters* **17,** 991 (1966).
J. COOPER, *Rev. Mod. Phys.* **39,** 167 (1967).
A. R. EDMONDS, *Angular Momentum in Quantum Mechanics*, Princeton University Press, Princeton, New Jersey (1960).
F. N. EDMONDS, H. SCHLÜTER and D. C. WELLS, *Mem. R. astr. Soc.* **71,** 271 (1967).
R. C. ELTON and H. R. GRIEM, *Phys. Rev.* **135,** A1550 (1964).
E. FERGUSON and H. SCHLÜTER, *Ann. Phys.* **22,** 351 (1963).
J. B. GERARDO and R. A. HILL, *Phys. Rev. Lett.* **17,** 623 (1966).
H. R. GRIEM, A. C. KOLB and K. Y. SHEN, *Phys. Rev.* **116,** 4 (1959).
H. R. GRIEM, *Astrophys. J.* **136,** 422 (1962).
H. R. GRIEM, A. C. KOLB and K. Y. SHEN, *Astrophys. J.* **135,** 272 (1962).
H. R. GRIEM, *Phys. Rev.* **140,** A1140 (1965).
H. R. GRIEM, *Astrophys. J.* **147,** 1092 (1967).
H. R. GRIEM, *Astrophys. J.* **148,** 547 (1967).
C. F. HOOPER, *Phys. Rev.* **165,** 215 (1968).
C. F. HOOPER, *Phys. Rev.* **169,** 193 (1968).
J. W. B. HUGHES, *Proc. phys. Soc.* **91,** 810 (1967).
P. KEPPLE and H. R. GRIEM, *Phys. Rev.* **173,** 317 (1968).
M. LEWIS, *Phys. Rev.* **121,** 501 (1961).
E. MERZBACHER, *Quantum Mechanics*, Chap. 16, John Wiley, New York (1961).
H. PFENNIG, E. TREFFTZ and C. R. VIDAL, *JQSRT* **6,** 557 (1966).
H. PFENNIG and E. TREFFTZ, *Z. Naturforsch.* **21a,** 697 (1966).
H. PFENNIG, *Z. Naturforsch.* **21a,** 1648 (1966).
H. SCHLÜTER and C. AVILA, *Astrophys. J.* **144,** 785 (1966).
K. Y. SHEN and J. COOPER, *Astrophys. J.* **155,** 37 (1969).
E. W. SMITH and C. F. HOOPER, *Phys. Rev.* **157,** 126 (1967).
E. W. SMITH, C. R. VIDAL and J. COOPER, *J. Res. Natn. Bur. Stand.* **73A,** 389 (1969).
E. W. SMITH, C. R. VIDAL and J. COOPER, *J. Res. natn. Bur. Stand.* **73A,** 405 (1969).
E. W. SMITH, J. COOPER and C. R. VIDAL, *Phys. Rev.* **185,** 140 (1969).
A. UNSÖLD, *Physik der Sternatmosphären*, Springer, Berlin (1955).
H. VAN REGEMORTER, *C.r. heb. Seanc. Acad. Sci., Paris* **259,** 3979 (1964).
C. R. VIDAL, *Z. Naturforsch.* **19a,** 947 (1964).

C. R. VIDAL, *Proc. 7th Int. Conf. Phenomena in Ionized Gases*, p. 168, Belgrade (1965).
C. R. VIDAL, J. COOPER and E. W. SMITH, *NBS Monograph* **116** (1970).
D. VOSLAMBER, *Z. Naturforsch.* **24a,** 1458 (1969).
B. WENDE, *Z. Angew. Phys.* **22,** 181, 1967.

APPENDIX

THE LARGE TIME LIMIT OF THE THERMAL AVERAGE $\bar{F}(t)$

In equation (IX.31) the large time limit of the thermal average has been given, which is of the form

$$\bar{F}(t)_{t\to\infty} = At(B-\ln(4C^2)). \tag{1}$$

This form has been obtained by most modern impact theories. The additive constant B varies depending on what type of cutoff has been used. In the following we derive the different constants B for the different cutoff procedures which have been used and compare them with the numbers given in the literature.

The various methods to evaluate $\bar{F}_\infty$, the large time limit of $\bar{F}(t, n_k, n_e, T)$, differ essentially in three respects, namely by the upper and lower limits of the ρ-integral and by the limits of the t'-integral in equation (VIII.4). Based on the completed collision assumption (BARANGER, 1962), the limits of the latter integral are usually extended from $-\infty$ to $+\infty$. This approach, however, is not quite consistent with the cutoff at the Debye length, which would rather require the integral to go from $-T$ to $+T$ as done in this paper (T is defined by equation (IX.7)). We therefore have to investigate the following integrals:

$$\text{for} \int_0^t PV_c(t')\,dt' \to \int_{-T}^{+T} PV_c(t')\,dt' \qquad \text{(Case A)}$$

$$\bar{F}^a_\infty = 2\pi n_e(a\cdot D)^2 v_{av} t \int_0^\omega du \frac{4}{\sqrt{\pi}} u^3 e^{-u^2} \int_{x_{min}}^1 dx\, x\left[\cos\left(\frac{2C}{axu}\sqrt{(1-x^2)}\right)-1\right] \tag{2}$$

and

$$\text{for} \int_0^t PV_c(t')\,dt' \to \int_{-\infty}^{+\infty} PV_c(t')\,dt' \qquad \text{(Case B)}$$

$$\bar{F}^b_\infty = 2\pi n_e(a\cdot D)^2 v_{av} t \int_0^\infty du \frac{4}{\sqrt{\pi}} u^3 e^{-u^2} \int_{x_{min}}^1 dx\, x\left[\cos\left(\frac{2C}{axu}\right)-1\right] \tag{3}$$

where

$$x_{min} = \rho_{min}/(a\cdot D). \tag{4}$$

The factor $a = \rho_{max}/D$ is usually taken to be one and has in some papers (e.g. GRIEM *et al.*, 1962) been varied to 1.1 or to 0.606 as proposed by CHAPPELL, COOPER and SMITH, 1969. As a lower cutoff we consider in particular the three cases of $\rho_{min} = 0$, $\rho_{min} = \lambda$ and $\rho_{min} = 3(nq - n'q')\lambda = 2CD/u$ by setting

$$x_{min} = \frac{b}{a}\cdot\frac{2C}{u}. \tag{5}$$

In the following we will set $a = 1$. In order to recover the dependence on the upper cutoff parameter a, we only have to replace in all the following relations C by C/a. First of all, one realizes that with $x_{min} \le 1$ the lower limit on the u-integral is given by

$$u_0 = b\cdot 2C. \tag{6}$$

Hence, we have to evaluate the following two integrals

$$I^a = \int_{u_0}^\infty du\, u^3\, e^{-u^2} \int_{u_0/u}^1 dx\, x\left[\cos\left(\frac{2C}{xu}\sqrt{(1-x^2)}\right)-1\right] \tag{7}$$

and

$$I^b = \int_{u_0}^\infty du\, u^3\, e^{-u^2} \int_{u_0/u}^1 dx\, x\left[\cos\left(\frac{2C}{xu}\right)-1\right]. \tag{8}$$

The second integral can be simplified after a change of variables and a partial integration to

$$I^b = \frac{1}{2}\int_{u_0}^{\infty} u\,\mathrm{e}^{-u^2}\left[\cos\left(\frac{2C}{u}\right)-1\right]\mathrm{d}u. \tag{9}$$

After expanding the cosine and another change of variables we have

$$I^b = \frac{u_0^2}{4}\sum_{k=1}^{\infty}\frac{(-1)^k}{(2k)!}\left(\frac{2C}{u_0}\right)^{2k}\int_1^{\infty}\frac{\mathrm{e}^{-u_0^2 z}}{z^k}\,\mathrm{d}z \tag{10}$$

which can be expressed in terms of exponential integrals

$$I^b = -\frac{C^2}{2}E_1(u_0^2)+\frac{u_0^2}{4}\sum_{k=2}^{\infty}\frac{(-1)^k}{(2k)!}\left(\frac{2C}{u_0}\right)^{2k}E_k(u_0^2). \tag{11}$$

With the lower cutoff parameters stated above ($b \le 1$) and typical densities and temperatures of interest one usually has $u_0 < 0.1$ (see equation (IX.21)). Since for $k \ge 2$, $E_k(u_0^2) = 1/(k-1)+0(u_0^2)$ one obtains to lowest order in u_0^2

$$\begin{aligned} I^b &= \frac{C^2}{2}\left[-E_1(u_0^2)+2\sum_{k=2}^{\infty}\frac{(-1)^k}{(2k)!}\left(\frac{2C}{u_0}\right)^{2k-2}\frac{1}{k-1}\right] \\ &= \frac{C^2}{2}\left[-E_1(u_0^2)+2\sum_{k=2}^{\infty}\left\{\frac{1}{(2k)!}+\frac{1}{(2k-1)!}-\frac{1}{(2k-2)(2k-2)!}\right\}\left\{-\frac{4C^2}{u_0^2}\right\}^{k-1}\right] \\ &= \frac{C^2}{2}\left[-E_1(u_0^2)-2\left(\frac{u_0}{2C}\right)^2\left\{\cos\left(\frac{2C}{u_0}\right)+\frac{1}{2}\left(\frac{2C}{u_0}\right)^2-1\right\}\right. \\ &\quad \left.+2\left(\frac{u_0}{2C}\right)\left\{\sin\left(\frac{2C}{u_0}\right)-\left(\frac{2C}{u_0}\right)\right\}-2\left\{\mathrm{Ci}\left(\frac{2C}{u_0}\right)-\gamma-\ln\left(\frac{2C}{u_0}\right)\right\}\right], \end{aligned} \tag{12}$$

which yields

$$I^b = \frac{C^2}{2}\left[3(\gamma-1)+\ln(4C^2)+2K\left(\frac{1}{b}\right)+0(u_0^2)\right] \tag{13}$$

where K is defined as

$$K(z) = \frac{1-\cos z}{z^2}+\frac{\sin z}{z}-\mathrm{Ci}(z) \tag{14}$$

and Ci is the cosine integral. Equation (13) was obtained already by SHEN and COOPER, 1969. Their constant A is identical with our constant $2C$.

The other integral I^a of equation (7) one can obtain by evaluating

$$\Delta I = \int_{u_0}^{\infty}\mathrm{d}u\,u^3\,\mathrm{e}^{-u^2}\int_{u_0/u}^{1}\mathrm{d}x\,x\left[\cos\left(\frac{2C}{ux}\sqrt{(1-x^2)}\right)-\cos\left(\frac{2C}{ux}\right)\right] \tag{15}$$

so that

$$I^a = I^b+\Delta I. \tag{16}$$

If we again expand the cosine functions, ΔI can be given by

$$\begin{aligned} \Delta I &= \sum_{k=1}^{\infty}\frac{(2C)^{2k}}{(2k)!}\sum_{j=0}^{k-1}\frac{k!(-1)^j}{j!(k-j)!}\int_{u_0}^{\infty}\mathrm{d}u\,u^{3-2k}\,\mathrm{e}^{-u^2}\int_{u_0/u}^{1}x^{1-2j}\,\mathrm{d}x \\ &= \frac{C^2}{2}\left[\mathrm{e}^{-u_0^2}-u_0^2E_1(u_0^2)\right] \\ &\quad +\frac{C^2}{2}2u_0^2\sum_{k=2}^{\infty}\frac{1}{(2k)!}\left(\frac{2C}{u_0}\right)^{2k-2}\left[E_{k-1}(u_0^2)-E_k(u_0^2)-k\int_1^{\infty}e^{-u_0^2 z}\frac{\ln z}{z^{k-1}}\,\mathrm{d}z\right] \\ &\quad -\frac{C^2}{2}4u_0^2\sum_{k=3}^{\infty}\frac{k!}{(2k)!}\left(\frac{2C}{u_0}\right)^{2k-2}\sum_{j=2}^{k-1}\frac{(-1)^j}{j!(k-j)!(2j-2)}\left[E_{k-1}(u_0^2)-E_{k-j}(u_0^2)\right] \end{aligned} \tag{17}$$

which gives us to lowest order in u_0^2

$$\Delta I = \frac{C^2}{2}\left[1+O(u_0^2)\right]. \tag{18}$$

This means that for the same lower cutoff Case A and B as defined in the equations (2) and (3) differ only by a constant 1 in their additive constant B. As a result we have

$$\bar{F}_\infty = -\left\{\frac{3}{2}(nq-n'q')\frac{\hbar}{m}\right\}^2 n_e t \sqrt{\left(\frac{8\pi m}{kT}\right)}[B-\ln(4C^2)] \tag{19}$$

where the constant B for the different cutoff parameters is compiled in the following Table 2.

TABLE 2. THE CONSTANT B FOR DIFFERENT CUTOFF PARAMETERS

	$\int_{-T}^{+T} PV_c(t')\,dt'$	$\int_{-\infty}^{+\infty} PV_c(t')\,dt'$
$\rho_{min} = 0$	0.27	1.27
$\rho_{min} = \lambda\!\!\!^{-}$	$0.23 \rightarrow 0.27$	$1.23 \rightarrow 1.27$
$\rho_{min} = 3n_k\lambda\!\!\!^{-}$	-1.66	-0.66

In order to compare our results with the numbers given in the literature we rewrite equation (19) as

$$\bar{F}_\infty = -A \cdot t \cdot [B_0 - \gamma - \ln(y_{min})] \tag{20}$$

where y_{min} as introduced by GRIEM, KOLB and SHEN (GRIEM *et al.*, 1959) is given by

$$y_{min} = \frac{4\pi n_e}{3m}\left(\frac{e\hbar n^2}{kT}\right)^2 = \frac{2}{3}\left(\frac{n^2}{3(nq-n'q')}\right)^2 4C^2. \tag{21}$$

Consequently, B and B_0 are related by the following relation

$$B_0 = B+\gamma+\ln\left[\frac{2}{3}\left(\frac{n^2}{3n_k}\right)^2\right]. \tag{22}$$

Comparing equations (19) and (20) one notices that for a particular line the value of the square bracket as derived here depends on the quantum number n_k for that particular state. This is also true for the paper of SHEN and COOPER, 1969, who consider our case (b) with infinite limits on the t'-integral. Otherwise the constants given in the literature are independent of n_k because the lower cutoff parameter is usually based on an average Stark splitting. If we set $nq-n'q' = n^2/2$, which corresponds approximately to the average Stark splitting and also gives the results for the Stark shifted component of Lyman-α, we have

$$B_0 = B-0.64. \tag{23}$$

This yields directly for $n_k = n^2/2$ the B_0 values corresponding to the B values in Table 2.

The following constants B_0 have been given in the literature:

GRIEM, KOLB and SHEN, 1959; (equation 29):	$B_0 = 0$
GRIEM, KOLB and SHEN, 1962; (equation 2):	$B_0 = 1.0$
GRIEM, 1965 KEPPLE and GRIEM, 1968 (neglecting quadrupole term):	$B_0 = 0.58$
SHEN and COOPER, 1969;	$B_0 = 0.58$

Recently the time development operator (S-matrix) has been evaluated for Lyman-α including time ordering by solving the differential equations for the S-matrix elements (BACON, 1969). Again the square bracket depends on $(nq-n'q')$ and the average value $B_0 = 1.1$ considering only the dipole term. It should, however, be stressed that one should not overinterpret these numbers because within the classical path approximation there is always some uncertainty about the "correct" constant B because of the ambiguous lower cutoff. This is due to the fact that the classical path approximation breaks down roughly for $\rho \gtrsim \lambda\!\!\!^{-}$ (for details see paper I). For most cases this has no significant effect for the Stark broadening of hydrogen because the *dynamic* broadening is primarily due to weak collisions. More details are given with the discussion at the end of Chapter XII. The situation is quite different for the broadening of ionized lines where strong collisions are very important and where the uncertainty of the classical path approximation accounts for part of the still existing discrepancies between theory and experiment, which are large compared with the Stark broadening of hydrogen.

So far we have considered $\bar{F}_\infty$, which is the basis of the unmodified impact theory. In order to extend the range of validity beyond the plasma frequency the modified impact theory introduces the Lewis cutoff by considering only those collisions for which the duration of a collision, which is typically ρ/v, is smaller than the time

of interest being typically $1/\Delta\omega$. For this reason the modified impact theory introduces an upper cutoff

$$\rho_{\max} = \mathrm{MIN}(D, v_{\mathrm{av}}/\Delta\omega) \tag{24}$$

or

$$\rho_{\max}/D = \mathrm{MIN}(1, 1/\Delta\omega_R).$$

It should be noted at this stage that in the following relations we not only have to replace C by C/a but also $\Delta\omega_R$ by a $\Delta\omega_R$, in order to obtain the dependence on the upper cutoff parameter a. Considering the usually applied case (b) (equation (3)) we have to evaluate the following integral for $\Delta\omega_R > 1$

$$I_L^b = \int_{u_0\Delta\omega_R}^{\infty} \mathrm{d}u\, u^3\, \mathrm{e}^{-u^2} \int_{u_0/u}^{1/\Delta\omega_R} \mathrm{d}x\, x\left[\cos\left(\frac{2C}{xu}\right) - 1\right] \tag{25}$$

where the lower limit on the u-integral is determined by the condition $u_0/u \leq 1/\Delta\omega_R$. After a change of variables and a partial integration one obtains similar to equation (9)

$$I_L^b = \frac{1}{2\Delta\omega_R^2} \int_{u_0\Delta\omega_R}^{\infty} u\, \mathrm{e}^{-u^2}\left[\cos\left(\frac{2C\Delta\omega_R}{u}\right) - 1\right] \mathrm{d}u. \tag{26}$$

Expanding the cosine again and performing another change of variables the result is

$$I_L^b = \frac{u_0^2}{4} \sum_{k=1}^{\infty} \frac{(-1)^k}{(2k)!}\left(\frac{2C}{u_0}\right)^{2k} \int_1^{\infty} \frac{\mathrm{e}^{-u_0^2\Delta\omega_R^2 z}}{z^k}\, \mathrm{d}z. \tag{27}$$

This gives us then

$$I_L^b = -\frac{C^2}{2} E_1(u_0^2\Delta\omega_R^2) + \frac{u_0^2}{4} \sum_{k=2}^{\infty} \frac{(-1)^k}{(2k)!}\left(\frac{2C}{u_0}\right)^{2k} E_k(u_0^2\Delta\omega_R^2). \tag{28}$$

Evaluating the exponential integrals E_k for small arguments only we finally have

$$\begin{aligned} I_L^b &= \frac{C^2}{2}[-E_1(u_0^2\Delta\omega_R^2) + E_1(u_0^2)] + I^b \\ &= C^2 \ln \Delta\omega_R + I^b \end{aligned} \tag{29}$$

which gives us for $\Delta\omega_R > 1$ the log-dependence of the Φ_{ab}-matrix elements in the modified impact theory. A more appropriate way for applying the Lewis cutoff, which avoids the discontinuity at $\Delta\omega_R = 1$, is to take as an upper cutoff $\rho_{\max} = \mathrm{MIN}(D, v/\Delta\omega)$. This case is worked out in the Appendix B of the report of VIDAL, 1970.

Similar results can be obtained for Case A, which are not included because they are no longer required. The derivation for Case B has been included, in order to obtain consistent relations which allow a comparison with the calculations done in this paper. The results for Case B as given here differ slightly from the results in the literature which also vary from paper to paper depending on the average matrix elements used and on what lower cutoff and average velocity has been applied.